Fall 2023 PHYS1494UN Physics Lab Reports Comiled

Tiffany Fu

January 9, 2024

Finding velocity, acceleration, and g with a Frictionless Inclined Plane (Revised Sep 2023)

Tiffany Fu, Anvita Bansal, Alexandria Lam

1 Introduction

Gravity is constantly weighing us down. It is something we can easily see – like an apple falling off a tree. But calculating the nominal value of the gravitational constant proves much more difficult than a simple observation. Yet, an accurate value of g is a fundamental constant needed for discovering the physical world.

In this experiment we are given a inclined plane and motion detector. The question we pose is how can we – like Galileo centuries ago– use these simple tools to calculate an accurate value of g. In our method we created a level plane by ensuring a consistent velocity after collision and then added a series of five different heights to incline the plane. In completing multiple trials we were able to calculate a g constant over all trials by the derivation of mechanics equations. In the conclusion the of our experiment and data analyses we observed an acceleration constant of 5.514 m/s^2.

2 Method

Our procedure includes a concise set of instruments – an air track, rider, motion detector, sonic ranger, and computer. The air track is setup with elastic bands on both ends and acted as an inclined plane when metal slabs were placed beneath one side of the track. The sonic ranger was placed on the side of the track pointing along the tracks central axis. The detector was plugged into a computer using DataStudio to collect trial data. Below is a simple diagram of our experimental setup.

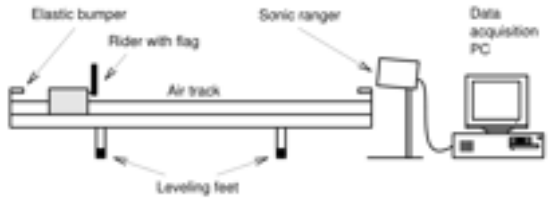

Figure 1.1: Setup of air track and PC.

After testing and ensuring a level air-track, we use five thin metal slabs to incline the track to five different heights. At each height we take 10 trials placing the rider on the 150cm position of the air track and then releasing. We began collecting data, position and velocity, when the rider collided with the elastic for the first time and stopped after its second collision.

3 Results & Analysis

Our first step of analysis is observing the coefficient of restitution during our constant velocity portion of our experiment – the level track. The coefficient of restitution e_j is calculated by the absolute value of final velocity divided by the initial velocity.

$$e_j = \left| \frac{v_f}{v_i} \right|$$

Then, for each 10 values of e_j we calculate the uncertainty σ_{e_j} by propagating errors using the following equation.

$$\sigma_{e_j} = \sqrt{\left(\frac{\partial e}{\partial v_i}\right)^2 \sigma_{v_i}^2 + \left(\frac{\partial e}{\partial v_f}\right)^2 \sigma_{v_f}^2}$$

Fig. 1: Standard Deviation of e_j

This equation can be simplified by taking the partial derivative.

$$\sigma_{e_j} = \sqrt{\left(-\frac{v_f}{v_i^2}\right)^2 \sigma_{v_i}^2 + \left(\frac{1}{v_i}\right)^2 \sigma_{v_f}^2}$$

Fig. 2: Simplified Standard Deviation equation

Our resulting coefficients of restitution and uncertainty are as follows:

e_j	σ_{e_j}
0.922	0.0032
0.939	0.0026
0.976	0.0046
0.941	0.0031
0.952	0.0095
1.004	0.0098
0.951	0.0304
0.929	0.0027
0.993	0.0142
0.972	0.0105

Tab. 1: Coefficients of Restitution

Next, we will calculate the unweighted mean $\bar{e}$ and standard error on the mean $\sigma_{\bar{e}}$.

$\bar{e}$	$\sigma_{\bar{e}}$
0.958	0.0087

Tab. 2: Unweighted Mean

Finally, we calculate the weighted mean $\bar{e}_w$ and standard error $\sigma_{\bar{e}_w}$.

$\bar{e}_w$	$\sigma_{\bar{e}_w}$
0.940	0.0013

Tab. 3: Weighted Mean

1. The weighted mean (0.940) is less than the unweighted mean (0.958). The standard deviation of the weighted mean (0.00132) is less than the unweighted mean (0.00865).

2. This **does agree** with our expectations. We expect the coefficient of restitution to not correlate with the initial velocity; instead it correlates with the amount of friction on the track and the elasticity of the collision.

3. The uncertainties in v_i and v_f are truly independent. The initial velocity is calculated by finding the slope of the location values for the cart before the collision. The final velocity is calculated by finding the slope of the location values for the cart after the collision. These are calculated from different sets of data (before and after the collision), so they should not affect each other.

4. The values of e do appear to be randomly distributed about the unweighted and weighted mean. By observing this plot, it can be seen that e is more evenly distributed about the unweighted mean than the weighted mean.

Gravitational Acceleration

Now we will estimate g by analyzing our acceleration data.

$h(mm)$	$\bar{a}_x$	$\sigma_{\bar{a}_x}$
1.2	0.0178	0.00143
2.6	0.0201	0.01007
4.0	0.0245	0.00537
5.3	0.0383	0.00810
6.8	0.0427	0.00224

Tab. 4: $h(mm)$, $\bar{a}_x$, and $\sigma_{\bar{a}_x}$

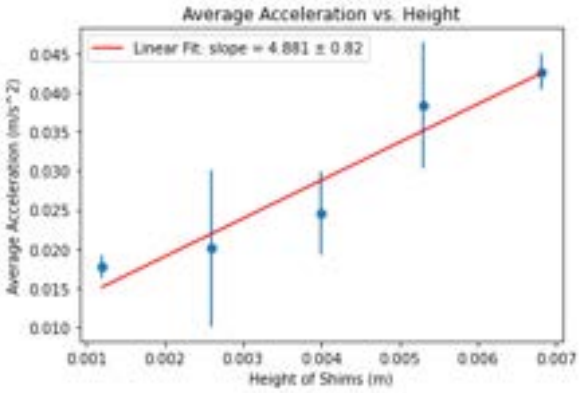

Fig. 3: $\bar{a}_x$ vs. $h(m)$ plot with error bars and linear fit

$$\bar{a}_x = 4.88h + 0.820$$

Our error for slope was 0.820.

Next, because we consider $a_x = \left(\frac{g}{L}\right) h$, we can estimate g with our calculated slope. L is average of the measured distances traveled by the rider – 1.13 meters.

$$a_x = \left(\frac{g}{L}\right) h = mh$$
$$a_x = \left(\frac{g}{1.13}\right) h = (4.88)h$$
$$\frac{g}{1.13} = 4.88$$
$$g = 4.88 * 1.13 = 5.514$$

1. Our measurement of g – 5.514 m/s^2 – does not agree with the nominal value of 9.80 m/s^2. Our calculated value is about four standard deviations from the expected value therefore it cannot be explained by natural variation in g.

2. Our intercept was 0.820 which is a statistically significant difference from 0. This could be caused by errors in our acceleration measurements resulting a less accurate line of best fit.

3. We expect steeper slopes to be more accurate for extracting g because it would suggest a less significantly different from 0 intercept. Our results are consistent with this, since our slope was shallow, we had a statistically different intercept resulting in a less accurate evaluation of g.

4. Friction from the track exerted on the rider is a systemic effect that may have been at work in this experiment. Our estimation on frictional loss calculated in the following section is evidence on its impact on our results.

5. Because the plane was not perfectly frictionless, there are limits in our experiments precision of measuring g. A pendulum measurement is more precise because no energy is dissipated due to friction and therfore a more precisce measurement of acceleration can be observed considering the conservation of energy. To improve precision in this experiment we cold implement a machine to release the rider in order to eliminate possible work added by a human release. Additionally using a machine to lift the plane could help better ensure consistent heights. Finally, recording more trials would also further increasing the precision of our results.

Estimating Friction Loss
In this section we will observe the energy lost due to friction during our experiment. Using the following equation we compute the friction loss of a couple trials from each height of our procedure.

$$\Delta = \frac{v_1^2}{2a_x l_2} - 1$$

h	Δ
1.2	-0.108
	-0.143
2.6	-0.089
	-0.163
4.0	-0.235
	-0.233
5.3	-0.391
	-0.349
6.8	-0.340
	-0.373

Tab. 5: height and friction loss

4 Conclusion

In this experiment, we were motivated to use simple tools to observe a nominal value of little g. Using an inclined plane, rider, and motion detector we recorded velocity, acceleration, and distance traveled for numerous trials. After completing a straight-foward data analysis, we concluded with a gravitation constant of 5.514 m/s^2. While this does not align our with expected nominal value of 9.8, we note several opportunities for improvement in our experiment including taking more trials and having a more precise release procedure. Nevertheless, going through the process of calculating a value of g is an important lesson that will pave the way for all other physical discoveries to follow.

5 Code

```
import matplotlib.pyplot as plt
import pandas as pd
import numpy as np


# Generate sample data
data = pd.read_csv('labreport1data.csv')
x = data['h(m)']
y = data['unweighted mean a (m/s^2)']
y_error = data['uncertainty a']

# Fit a linear regression line
slope, intercept = np.polyfit(x, y, 1)
fit_line = slope * x + intercept

# Create a scatter plot with error bars
plt.scatter(x, y)
plt.errorbar(x, y, yerr=y_error, linestyle='')

# Plot the linear fit
plt.plot(x, fit_line, color='red', label='Linear Fit: slope = 4.881 ± 0.82')

# Add labels and legend
plt.xlabel('Height of Shims (m)')
plt.ylabel('Average Acceleration (m/s^2)')
plt.legend(loc='upper left')

# Show the plot
plt.show()
```

Projectile Motion and Conservation of Energy (Revised Sep 2023)

Author: Tiffany Fu / Lab Members: Anvita Bansal, Alexandria Lam

1 Introduction

To me, the magic of physics is being able predict real world behaviors by using and transforming simple mathematical equations. In this lab we go through the procedure of prediction by specifically observing two-dimensional free fall and projectile motion. Using mechanical trajectory equations we derive an equation to predict the range traveled by a marble launched through an experimental apparatus. We go through this derivation in our methods section to result in an equation with six measurement parameters.

For the experiment, we set up the tube apparatus and record the height measurements. Using our equation and measurements, we get the predicted distance and place a paper with crosshairs and a carbon sheet on top at the predicted location. We take 20 trials rolling the ball through the apparatus and letting it land on our paper. We do two configurations for both a metal ball and plastic ball.

In our data analysis, we observe and compare the predicted and observed means and spreads. In the result of our experiment, our predicted and mean positions agreed within uncertainties. We also noted some systemic errors which caused shifts in our data points from expected values.

2 Method

Our setup is a tube apparatus with a release point, pivot, and launch point.

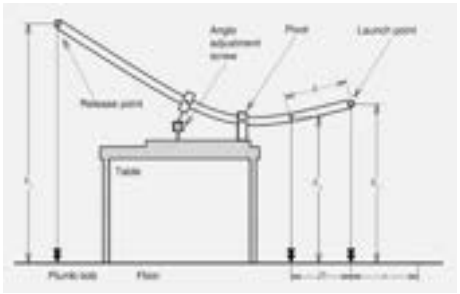

Fig. 1: Experimental Setup

Before be begin our experimental procedure, we must derive an expression predicting the distance the ball will travel given the parameters h_1, h_2, h_3, D, L, and $\Delta h'$. We break down this derivation into the following steps.

1. Find v_0 using the conservation of total mechanical energy and energy lost due to friction.

$$E_{\text{kin}}^{\text{in}} + E_{\text{pot}}^{\text{in}} = E_{\text{kin}}^{\text{fin}} + E_{\text{pot}}^{\text{fin}} + W_f$$

$$0 = \Delta E_{\text{kin}} + \Delta E_{\text{pot}} - W_f$$

Kinetic energy is calculated by the sum of translational and rotational kinetic energy.

$$E_{\text{kin}} = E_{\text{transl}} + E_{\text{rot}} = \frac{1}{2}mv^2 + \frac{1}{2}I\omega^2$$

$$= \frac{1}{2}mv^2 + \frac{1}{2}I\left(\frac{v_0}{R}\right)^2 = \boxed{\frac{7}{10}mv_0^2}$$

Fig. 2: Derivation of Change in Kinetic Energy

The potential energy is associated with the presence of a gravitational field. The expression for an object's potential energy near the surface of the Earth is expressed as:

$$E_{\text{pot}}(r) = -G_N\frac{M_E m}{r} \simeq mgh$$

For the experiment, the total difference in potential energy is the difference in potential energy from the release and launch point.

$$\Delta E_{\text{pot}} = mg(h_1 - h_2) = mg\Delta h$$

Fig. 3: Derivation of Change in Potential Energy

When we set up the procedure at h_1 and h_2 the velocity of the marble at the release and launch point are zero, in other words the change in potential energy is 0. Applying this to the conservation of momentum equation we derivate the work done by friction.

$$\Delta E_{\text{kin}} + \Delta E_{\text{pot}} - W_f = \Delta E_{\text{pot}} - W_f = 0$$

$$W_f = mg(h_1' - h_2') = mg\Delta h'$$

Fig. 4: Derivation of Work due to Friction

Taking all equations together we derivate.

$$0 = \frac{7}{10}mv_0^2 + mg\Delta h - mg\Delta h'$$

$$\frac{7}{10}mv_0^2 = mg\Delta h' - mg\Delta h$$

$$\boxed{v_0 = \pm\sqrt{\frac{10}{7}g(\Delta h' - \Delta h)}}$$

Fig. 5: Derivation of Initial Velocity

2. Next, we find $v_{0,x}$ and $v_{0,y}$ by splitting up the initial velocity into its vertical and horizontal components.

$$v_{0,x} = v_0 cos\theta = v_0(D/L)$$

$$v_{0,y} = v_0 sin\theta = v_0(h_2 - h_3/L)$$

Fig. 6: Horizontal and Vertical components of initial velocity with experimental geometry

3. Now we will find the time of the marble in the air since we know the vertically acceleration is due to gravity.

$$h_2 + v_{0,y}t - \frac{1}{2}gt^2$$

We can solve for t by using the quadratic formula.

$$t = \frac{-v_{0,y} \pm \sqrt{v_{0,y}^2 - 4(-\frac{1}{2}g)(h_2)}}{2(-\frac{1}{2}g)}$$

$$\boxed{t = \frac{v_{0,y} \mp \sqrt{v_{0,y}^2 - 2gh_2}}{g}}$$

Fig. 7: Derivation for Time of Marble in Air

4. Finally, we can express the predicted range by putting all the pieces together.

$$x(t) = x_0 + v_{0,x}t = v_{0,x}t$$

$$v_0 = \sqrt{\frac{10}{7}g(\Delta h' - \Delta h)}$$

$$v_{0,x} = v_0(D/L) = \sqrt{\frac{10}{7}g(\Delta h' - \Delta h)}(D/L)$$

$$t = \frac{v_{0,y} + \sqrt{v_{0,y}^2 - 2gh_2}}{g}$$

$$= \frac{v_0(\frac{h_2 - h_3}{L}) + \sqrt{\left(v_0(\frac{h_2 - h_3}{L})\right)^2 - 2gh_2}}{g}$$

$$x(\Delta h', \Delta h, h_2, h_3, D, L, g) = \sqrt{\frac{10}{7}g(\Delta h' - \Delta h)}(D/L) \times \left(\frac{\sqrt{\frac{10}{7}g(\Delta h' - \Delta h)}\left(\frac{h_2 - h_3}{L}\right) + \sqrt{\left(\frac{10}{7}g(\Delta h' - \Delta h)\right)\left(\frac{h_2 - h_3}{L}\right)^2 - 2gh_2}}{g}\right)$$

Fig. 8: Final Equation for Predicted Distance Traveled by Marble

With this derivation, we will predict the distance traveled for four different arrangements. For the first two arrangements we will use a metal marble and then we will a plastic marble. Our predicted calculations with the given parameters are as follows.

	MB 1	MB 2	PB 1	PB 2
h_1	1.213	1.243	1.23	1.232
h_1'	1.184	1.184	1.18	1.202
h_2	1.150	1.136	1.13	1.134
h_2'	1.174	1.174	1.17	1.160
h_3	1.035	1.022	1.02	1.027
D	0.400	0.392	0.389	0.389
L	0.380	0.400	0.400	0.400
g	9.8	9.8	9.8	9.8
pred(m)	0.464	0.615	0.538	0.436

Tab. 1: Trial Configuration Measurements and Predicted Distance Traveled

With our predicted calculations we place a sheet of paper with crosshairs drawn at our predicted distance and cover it with a carbon sheet. For each trial/ configuration we conduct 20 observations, rolling the marble through the pipe and letting it bounce onto our sheet. Our resulting paper for Trial 1 is shown below. Each black dot represents one observation.

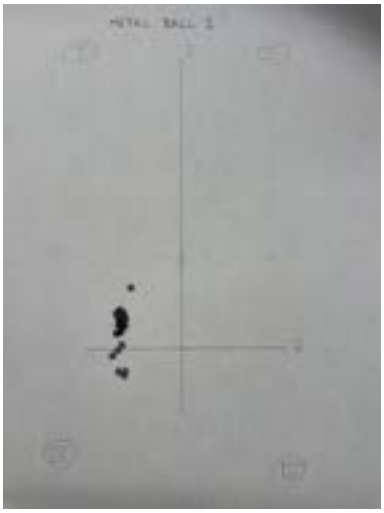

	$\bar{z}$ (cm)	$\bar{x}$ (cm)
1	-2.90	-1.30
2	-2.85	-1.13
3	-3.17	-1.10
4	-3.50	-0.30
5	-3.23	-0.10
...	...	...
15	-3.20	1.60
16	-2.98	1.80
17	-3.30	1.78
18	-3.10	1.80
19	-3.15	1.90
20	-2.60	3.05

Tab. 2: Marble 1 Observed x and z Positions

Next, we plot our results in histograms to better visualize our distribution of data.

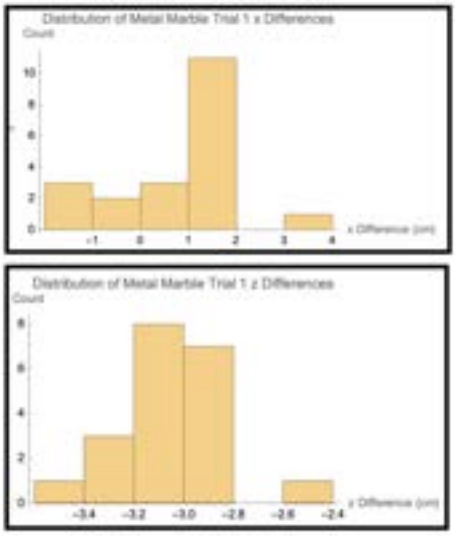

Fig. 9: Histograms of x and z Positional Differences for Metal Marble 1 Configuration

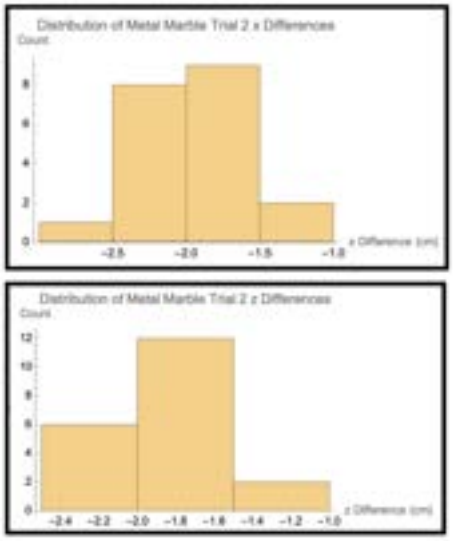

Fig. 10: Histograms of x and z Positional Differences for Metal Marble 2 Configuration

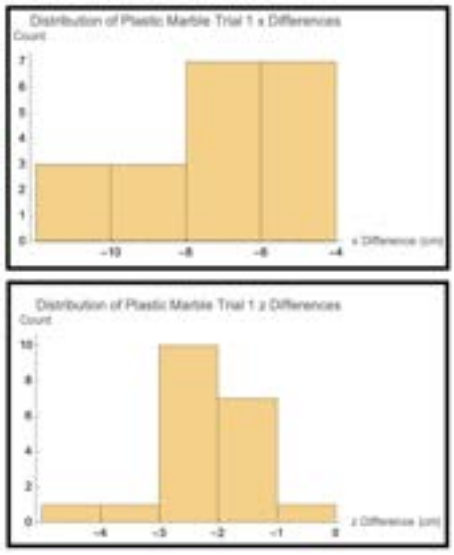

Fig. 11: Histograms of x and z Positional Differences for Plastic Marble 1 Configuration

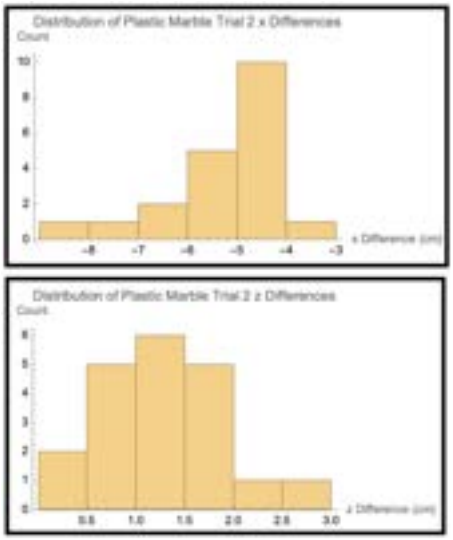

Fig. 12: Histograms of x and z Positional Differences for Plastic Marble 2 Configuration

3 Results & Analysis

Our first step of analysis is estimating the expected x distance traveled by the marble for each trial. We propagate the uncertainties in our measurements of $h1,\ h2,\ h3,\ L$,and D by taking partial derivatives of our equation for predicted range. To make the process less long and tedious we will utilize the given approximation.

$$x_{\text{approx}} = \frac{D\sqrt{2h_2h_E}}{L} \text{ , where } h_E = \frac{10}{7}(\Delta h - \Delta h')$$

$$\sigma_x^2 = \left(\frac{\partial x}{\partial h_2}\right)\sigma_{h_2}^2 + \left(\frac{\partial x}{\partial D}\right)\sigma_D^2 + \left(\frac{\partial x}{\partial L}\right)\sigma_L^2 + \left(\frac{\partial x}{\partial h_1}\right)\sigma_{h_1}^2 + \left(\frac{\partial x}{\partial h_1'}\right)\sigma_{h_1'}^2 + \left(\frac{\partial x}{\partial h_2'}\right)\sigma_{h_2'}^2$$

$$\frac{\partial x}{\partial D} = \frac{1}{L}\sqrt{\frac{20}{7}h_2(\Delta h - \Delta h'}$$
$$\frac{\partial x}{\partial D}^2 = \frac{1}{L^2}\left(\frac{20}{7}h_2(\Delta h - \Delta h')\right)$$

$$\frac{\partial x}{\partial L} = -\frac{2\sqrt{5}}{\sqrt{7}}\frac{D}{L^2}\sqrt{h_2(\Delta h - \Delta h')}$$
$$\frac{\partial x}{\partial L}^2 = -\frac{45}{7}\frac{D^2}{L^4}h_2(\Delta h - \Delta h')$$

$$\frac{\partial x}{\partial h_1} = \frac{D}{L}\frac{\sqrt{5h_2}}{\sqrt{7}\sqrt{\Delta h - \Delta h'}}$$
$$\frac{\partial x}{\partial h_1}^2 = \frac{5}{7}\frac{D^2}{L^2}\frac{h_2}{\Delta h - \Delta h'}$$

$$\frac{\partial x}{\partial h_2} = \frac{D}{L}\sqrt{\frac{5}{7}}\frac{-2h_2 + h_1 - h_1' + h_2'}{\sqrt{h_2(\Delta h - \Delta h')}}$$
$$\frac{\partial x}{\partial h_2}^2 = \frac{D^2}{L^2}\frac{5}{7}\frac{(-2h_2 + h_1 - h_1' + h_2')^2}{h_2(\Delta h - \Delta h')}$$

$$\frac{\partial x}{\partial h_1'} = \frac{D}{L}\sqrt{\frac{5}{7}}\frac{\sqrt{h_2}}{\sqrt{\Delta h - \Delta h'}}$$
$$\frac{\partial x}{\partial h_1'}^2 = \frac{D^2}{L^2}\frac{5}{7}\frac{h_2}{\Delta h - \Delta h'}$$

$$\frac{\partial x}{\partial h_2'} = \frac{D}{L}\sqrt{\frac{5}{7}}\frac{\sqrt{h_2}}{\sqrt{\Delta h - \Delta h'}}$$
$$\frac{\partial x}{\partial h_2'}^2 = \frac{D^2}{L^2}\frac{5}{7}\frac{h_2}{\Delta h - \Delta h'}$$

The uncertainty for measuring with a meter-stick is 1mm.

$$\sigma_h^2 = \sigma_D^2 = \sigma_L^2 = \sigma_{h_1}^2 = \sigma_{h_2}^2 = \sigma_{h_1'}^2 = \sigma_{h_2'}^2 = 0.1\text{cm}$$

Therefore, our final expression is as follows

$$\sigma_x^2 = \frac{1}{140}\frac{D^2}{L^2}\left(\frac{4h_2}{D^2}(\Delta h - \Delta h') + \frac{9}{L^2}h_2(\Delta h - \Delta h') + \frac{h_2^2}{\Delta h - \Delta h'} + \frac{(-2h_2 + h_1 - \Delta h')^2}{h_2(\Delta h - \Delta h')} + \frac{2h_2}{\Delta h - \Delta h'}\right)$$

Fig. 13: Final expression for Predicted Uncertainty

Next we will record the mean positions observed in both the x and z position and calculate experimental uncertainties using the following equations.

$$\bar{x} = \frac{1}{N}\sum_{i=1}^{N} x_i \ , \ \sigma_x = \sqrt{\frac{\sum(x_i - \bar{x})}{N-1}} \ , \ \sigma_{\bar{x}} = \frac{\sigma_x}{\sqrt{N}}$$

Fig. 14: Equations for means, standard deviations, and standard deviations of means

Our final results are as follows:

	MB 1	MB 2
pred (x)	0.464 ± 0.937	0.615 ± 0.436
obs (x)	0.465 ± 9.47E-4	0.613 ± 8.78E-5
obs (z)	-0.031 ± 0.004	-0.019 ± 0.004

Tab. 3: Resulting Calculations for Predicted x and Observed x, z Positions and Uncertainties

	PB 1	PB 2
pred (x)	0.538 ± 0.987	0.435 ± 1.517
obs (x)	0.531 ± 4.56E-4	0.431 ± 2.59E-4
obs (z)	−0.024± 0.005	-0.020 ± 0.001

Tab. 4: Resulting Calculations for Predicted x and Observed x, z Positions and Uncertainties

4 Discussion

1. All of our predicted and mean positions agree within uncertainties.
2. Though it is difficult to conclude with our small sample size, our histograms mostly seem randomly distributed however they are not centered on the expected value of 0.
3. Since there are overall shifts in data points we observe systematic errors in our experiment. One potential factor we observed is that our two-meter stick was not perfectly straight. If this is the case, all our measurements of heights and distances would create a systematically incorrect prediction. Another potential source of systematic error is since we could not clean the whole pipe materials in the tube may cause extra friction.
4. In most trials the spread along the x direction was similar to the spread long the z direction. This means variation was mostly due to natural variation.
5. The spreads are similar except in Metal Ball Trial 2 the spread is significantly less than the spread of the plastic marble trials. This makes since since a plastic ball is lighter and has less inertia making it more effected by natural variance from factors like wind.
6. To decrease spread in the experiment, a more precise measurement system could be implemented such as a laser plumbob and aluminum meterstick.
7. Since the moment of inertia for a hollow sphere is greater than a solid sphere, the predicted distance of travel would be less.
8. Systematic errors in our procedure limit the accuracy of our measurement of friction.
9. I estimate the length of the tube to be five times L by using L as a unit metric on the provided diagram. I expect this estimate to not be very accurate, a better method would have been measuring the tube with a measuring tape during the experiment. Nevertheless, we can get a sense of the magnitude of frictional force. Metal Ball (28.1 g):

   $$f_f = 28.1 * 9.8 * 0.01/(5 * 0.38) = 1.44\text{N}$$

   Plastic Ball (4.2g):

   $$f_f = 4.2 * 9.8 * 0.087/(5 * 0.40) = 1.79\text{N}$$

   Based on these calculations, we don't expect friction to be significant compared to other forces such as gravity.
10. If friction varies along the tube our estimate would not be as accurate. The magnitude of friction is determined by the material of the surface and mass of the object. I expect friction to be maximal at the pivot of the tube apparatus since the marble is in contact with the most surface area of the tube at this point.
11. We assume that the frictional effect of the tube is the same for the different configurations. We also assume that the velocity of the marble is 0 when released.

5 Conclusion

This lab demonstrated the predictive power of conceptual physics and natural laws. In our experiment we derive an expression to predict the distance traveled by a marble released and launched through the apparatus. We then compare predicted position to 20 observed positions for 4 configurations of the tube. After careful data analysis, we concluded that our observed and predicted means agreed within uncertainties.

Physical predictions are applied to real world situations to understand the motion and interacts of objects. The ability to make predictions using physics principles makes up the basis of how humans can manipulate objects to optimize efficiency and positive benefits.

6 Code

```
Histogram[{-2.9, -2.85, -3.17, -3.5, -3.23, -3, -3.28, -3.08, -2.91, -3, -3.2, -3.18, -3.1, -2.86, -3.2, -2.98, -3.3, -3.1, -3.15, -2.6},
 PlotLabel → "Distribution of Metal Marble Trial 1 z Differences", AxesLabel → {"z Difference (cm)", Count}]
```

```
Histogram[{-1.3, -1.13, -1.1, -0.3, -0.1, 0.2, 0.8, 0.85, 1.2, 1.21, 1.3, 1.5, 1.32, 1.5, 1.6, 1.8, 1.78, 1.8, 1.9, 3.05},
 PlotLabel → "Distribution of Metal Marble Trial 1 x Differences", AxesLabel → {"x Difference (cm)", Count}]
```

```
Histogram[{-1.2, -1.47, -1.6, -1.95, -2, -2.15, -2.21, -2.26, -2.3, -1.67, -1.55, -2.1, -1.85, -1.8, -1.95, -1.55,
  -1.85, -1.65, -1.8, -2.37}, PlotLabel → "Distribution of Metal Marble Trial 2 z Differences", AxesLabel → {"z Difference (cm)", Count}]
```

```
Histogram[{-1.65, -1.77, -1.88, -1.9, -1.86, -1.7, -1.45, -1.85, -1.55, -2.47, -2.3, -1.27, -2.4, -2.43, -1.8, -2.28,
  -2.43, -2.46, -2.55, -2.3}, PlotLabel → "Distribution of Metal Marble Trial 2 x Differences", AxesLabel → {"x Difference (cm)", Count}]
```

```
Histogram[{-2.72, -1.82, -1.92, -4.1, -1.85, -2.95, -2.88, -2.65, -1.4, -1, -2.85, -2.65, -2.97, -1.2, -2, -1.96,
  -2.46, -2.5, -2.93, -3.06}, PlotLabel → "Distribution of Plastic Marble Trial 1 z Differences",
 AxesLabel → {"z Difference (cm)", Count}]
```

```
Histogram[{-9.8, -10.72, -11.15, -11.9, -8.4, -8.3, -7.95, -7.6, -7.3, -7.2, -6.9, -6.85, -6.3, -6, -5.7, -4.95,
  -5.8, -5.55, -5.35, -5.7}, PlotLabel → "Distribution of Plastic Marble Trial 1 x Differences",
 AxesLabel → {"x Difference (cm)", Count}]
```

```
Histogram[{1.82, 2.6, 1.3, 1.8, 0.5, 0.3, 1.3, 1.35, 0.9, 0.85, 0.95, 1.25, 1.55, 0.45, 0.75, 1.2, 2.1, 1.25, 1.6, 1.55},
 PlotLabel → "Distribution of Plastic Marble Trial 2 z Differences", AxesLabel → {"z Difference (cm)", Count}]
```

```
Histogram[{-8.1, -7.4, -7, -6.1, -5.8, -5.65, -5.5, -5.35, -5.35, -4.95, -4.9, -4.76, -4.9, -4.97, -4.4, -4.55,
  -4.4, -4.1, -4.4, -3.32}, PlotLabel → "Distribution of Plastic Marble Trial 2 x Differences", AxesLabel → {"x Difference (cm)", Count}]
```

Magnetic Fields Lab (Revised Oct 2023)

Author: Tiffany Fu / Lab Members: Anvita Bansal, Alexandria Lam

1 Introduction

In 1820, physics professor Hans Christian Oersted discovered the hidden relationship between electricity and magnetism while casually setting up for his day's lecture. When a current traveling through a wire moved the needle of a nearby compass, Oersted's made an accidental discovery the incited the new field of electromagnetism. The outburst of research done by key figures in the following decades established the fundamental E and M equations.

Lorentz's law states that a force is created when a current interacts with a magnetic field.

$$\vec{F} = i\vec{L} \times \vec{B}$$

Fig. 1: Lorentz Force

Where i is current L is the length of the rod and B is the magnetic field strength.

A change in magnetic field can also create an induced EMF. In 1831 Michael Faraday derived the relationship between induced EMF and magnetic flux where magnetic flux is the amount of magnetic field going through a given area.

$$\Phi = \int \vec{B}\cdot\hat{n}dA, \quad \Phi = BA \text{ (if B and A are perpendicular)}$$

$$\varepsilon = -N\frac{d\Phi}{dt} = -NA\frac{\Delta B}{\Delta t}$$

Fig. 2: Faraday's Law

In the outlined experiment, we rediscover the relationships between electricity and magnetism by considering current through a wire, induced EMF, and magnetic field. In Part 1 we use a current to create a magnetic force that counter-balances the force of gravity acting on various weights. By analyzing our data we compute B-values for different electromagnetic power supplies and observe a positively linear relationship between B and I. In Part 2 we observe how a change in magnetic flux induces an EMF. Using an induction wand and a magnet we swing the wand through the magnetic field and record a graph of voltage. By analyzing this graph we record an EMF of 0.18 A. Using Faraday's formula and propagating for error, we calculated an ε of 0.295 ± 0.009 A.

2 Method

Our experiment involves two separate methods one involving current through a wire and the other involving a magnet and induced EMF.

Part 1

Our first setup includes an iron electromagnet and conducting bar connected to respective power supplies and a current balance with weights.

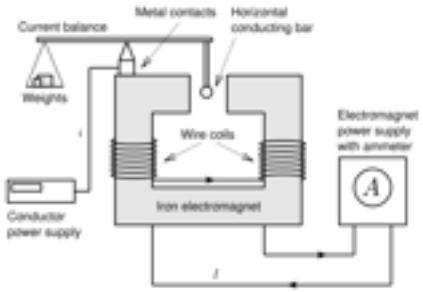

Fig. 3: Part 1 Experimental Setup

We begin by measuring the length of the conducting bar to be 34.9 mm. Then we set the electromagnet power supply to 4 ampmeters. We set a weight on the balance and let it tip. Then we turn on the conducting power supply and adjust the current knob until we observe a level balance using a mirror. We record the mass of the weight and value of the current and repeat this process for four different weights. When these five trials are completed we end with the following data.

Mass (g)	Current (A)
1.03	0.66
1.11	0.68
1.16	0.69
1.31	0.82
1.61	0.96

Tab. 1: Recorded weight and corresponding current placed through conductor (electromagnetic power supply of 4A).

Next, we repeat the process for different electromagnetic power supplies – namely 2.0A, 2.5A, 3.0A, and 3.5A. Table 2 summarizes our results.

Mass (g)	2.0 A	2.5 A	3.0 A	3.5 A	4.0 A
1.03	0.98	0.86	0.71	0.64	0.66
1.11	1.09	0.93	0.77	0.69	0.68
1.16	1.16	0.95	0.79	0.72	0.69
1.31	1.33	1.07	0.89	0.87	0.82
1.61	1.69	1.36	1.14	1.05	0.96

Tab. 2: Weights and current values through conductors for all electromagnetic power supplies.

Part 2

In this part of the experiment we observe magnetic field by induced EMF.

Our setup involves an induction coil and magnet generating a field. We have three sensors to record data a motion sensor, magnetic field sensor, and voltage sensor.

Fig. 4: Part 2 Experimental Setup

Firstly we will use the magnetic field sensor to measure the field strength of the magnet by placing it in the middle and using DataStudio. We observe a steady value of 0.0626 T for the magnetic field. Next we place the sensor 1cm from the center and 2cm from the center and note the values of B there. We observe the exponential decrease in field strength as distance increases.

	center	1 cm	2 cm
$B(T)$	0.0626	0.0607	0.0541

Tab. 3: Magnetic Field Strength of Magnet at Distances from Center.

Next, we place the magnet back in the setup so the coil can pass through. We release the wand allowing it to swing through once and record data on DataStudio. After the trial we end with the following graph.

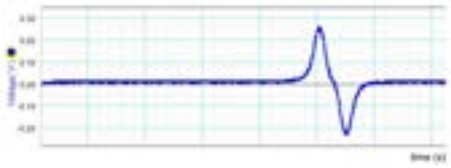

Fig. 5: Voltage in coil during one swing through Magnetic Field

Using Smart Tools we find the mean value of the first peak to be 0.18 A – this is our average EMF. The time difference between the beginning and end of the peak is 0.032 seconds.

3 Results, Analysis & Discussion

Part 1

Firstly, using out current balance data we will plot iL against $F = mg$.

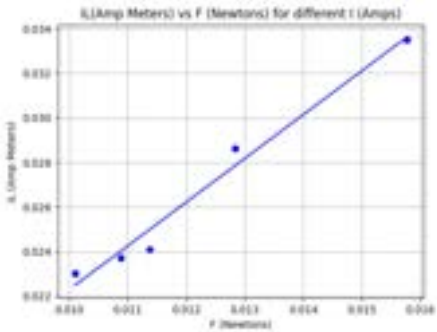

Fig. 6: iL versus F for trials with electromagnetic power supply of 4 A.

Using a linear least squares analysis we derive a slope of the plot and its corresponding uncertainty to be 1.961 and 0.0769 respectively. To find the magnetic field value we will take the reciprocal of the slope. To find the error of B we take its square.

$$iLB = F_g = mg$$
$$iL = slope(mg)$$
$$\frac{iL}{slope} = mg$$
$$B = \frac{mg}{iL} = \frac{1}{slope}$$

Fig. 7: Derived relationship between B and slope of linear regression.

Our resulting B-field for 4 A is 0.510 ± 0.020.

We repeat this process for our remaining trials and plot all graphs on one axis.

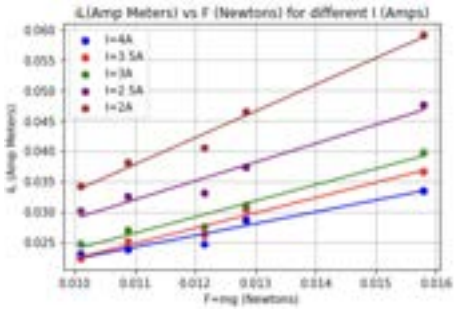

Fig. 8: Plot of iL against force values mg for all electromagnetic power supplies.

In summary, our values and uncertainties for magnetic field are as follows.

Current (A)	B (T)
2.0	0.510 ± 0.020
2.5	0.387 ± 0.010
3.0	0.380 ± 0.007
3.5	0.326 ± 0.007
4.0	0.232 ± 0.002

Tab. 4: Calculated magnetic field value and uncertainty for different experimental power supplies.

We plot I versus B to observe the relationship between the two variables.

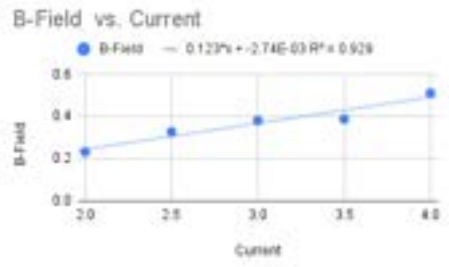

Fig. 9: Magnetic Field Values plotted against current with line of best fit.

The shape of this graph is positively linear. This makes sense because magnetic field strength is directly proportional to a current flowing through a long-straight wire as stated by Ampere's Law.

$$\int B \cdot dl = \mu_0 I$$

Fig. 10: Ampere's Law

So far we have observed the effect of current flowing through the horizontal bar. When we consider the current flowing through the two vertical bars of the apparatus we observe that the magnetic fields created through these parts cancel out due to current flowing down one bar and up the other bar.

Part 2

To calculate EMF we will use Faraday's equation with an N of 200, radius of 0.0155 m, ΔB of 0.0626 and Δt of 0.032 seconds.

$$\varepsilon = -NA\frac{\Delta B}{\Delta t} = 200(\pi(0.0155)^2)\left(\frac{0.0626}{0.032}\right)$$

Our calculated result is 0.295 A. We propagate error to get the uncertainty of this value to be 0.009.

$$\left(\frac{\sigma_\varepsilon}{\varepsilon}\right)^2 = \left(\frac{\sigma_N}{N}\right)^2 + \left(\frac{\sigma_{\Delta B}}{\Delta B}\right)^2 + \left(\frac{\sigma_{\Delta t}}{\Delta t}\right)^2$$

$$\left(\frac{\sigma_\varepsilon}{\varepsilon}\right)^2 = \left(\frac{\sigma_{\Delta B}}{\Delta B}\right)^2 + \left(\frac{\sigma_{\Delta t}}{\Delta t}\right)^2$$

$$\sigma_\varepsilon = 0.295\sqrt{\left(\frac{0.000001}{0.0626}\right)^2 + \left(\frac{0.001}{0.032}\right)^2}$$

$$\sigma_\varepsilon = \pm 0.009$$

Our observed value of 0.18 A and computed value of 0.295 A are not compatible within error. We note that this may be due to potential systematic errors such error in the induction wand or magnet.

Let's reintroduce our voltage graph with the time of the coil entering and leaving the magnet identified.

Fig. 11: Voltage versus time with entrance and departure identified.

We observe that the signs of the first peak and second peak differ. This is explained by the nature of the changing field through time. When the coil first swings and enters the magnet, there is a positive increase in magnetic field through the coils since field strength increases towards the center of the magnet. When it hits the center the EMF is zero because for a brief moment the field at the center of the magnet is steady and the change in B is zero. After the coil passes the center, the strength of the field decreases (as we first observed with the field sensor) this means that ΔB is the opposite sign than when it enters.

4 Conclusion

Oersted's discovery in 1820 opened up a Pandora's Box of experimental physics observing electromagnetic relationships. In this two-part experiment we used a current balance to observe the relationship between a current and magnetic force. We also utilized a conductor wand to observe an induced EMF due to changing magnetic flux. After careful data analysis, we calculated magnetic field values for five different electromagnetic power supply. When we plot current and magnetic field we observe a positively linear relationship explained by Ampere's Law. For part 2, we experimentally calculated an average EMF of 0.18 A and calculated a value of 0.295 using Faraday's Law.

Through this lab we have reinforced electromagnetic concepts. Through deeply understanding the relationships between electricity and magnetism we can now begin to predict behaviors and interactions of fundamental objects and ones that are not as easily observed as mechanical motion.

5 Code

```
import matplotlib.pyplot as plt
import numpy as np
from scipy.stats import linregress

iL4 = np.array([0.023034, 0.023732, 0.024081, 0.028618, 0.033504])
mg = np.array([0.010094, 0.010878, 0.011368, 0.012838, 0.015778])

plt.scatter(mg, iL4, color='blue')

slope1, intercept1 = np.polyfit(mg, iL4, 1)
plt.plot(mg, slope1 * mg + intercept1, color='blue')

slope1, intercept1, r_value1, p_value1, std_err1 = linregress(mg, iL4)

slope_error1 = std_err1 / np.sqrt(5)

print(f"4A: Slope = {slope1:.3f} ± {slope_error1:.5f}")

plt.ylabel('iL (Amp Meters)')
plt.xlabel('F (Newtons)')
plt.legend()
plt.title('iL(Amp Meters) vs F (Newtons) for different I (Amps)')

# Perform linear regression analysis for Line 4 A
slope1, intercept1, r_value1, p_value1, std_err1 = linregress(mg, iL4)

# Show the plot
plt.grid(True)
plt.show()
```

==

e/m of the Electron (Revised Oct 2023)

Author: Tiffany Fu / Lab Members: Anvita Bansal, Alexandria Lam

1 Introduction

For a long time, atoms were misunderstood and extremely elusive. How could we know so little about the things that fundamentally make up our world? It took several decades of scientific discovery before breakthroughs in atomic theory and models solidified. One major event in this timeline occurred in 1897 when JJ Thomson discovered the electron through an experiment involving cathode rays. This discovery disproved Dalton's atomic theory and propelled scientific discovery in atomic theory and models.

In our lab, we replicate Thomson's experiment using an apparatus consisting of Helmholtz coils creating a magnetic field, a cathode ray with an electron beam, and a ruler that allows us to record the diameter of the circular deflection. After gathering values for different voltages, magnetic fields, and radii, we are able to calculate the charge mass ratio using the following equation.

$$\frac{e}{m} = \frac{2V}{r^2B^2}$$

Fig. 1: Charge Mass Ration expressed by voltage, radius, and magnetic fields

We conclude our experiment with a value for charge-mass ratio of $1.93 * 10^{11}$ Ckg^{-1}.

2 Method

Before be begin the experiment, we derive an equation relating our measurements.

Using force equations we derive an equation for particle velocity.

$$\vec{F}_e = m\frac{v^2}{r} \qquad \vec{F}_{\text{mag}} = e\vec{v} \times \vec{B}$$

$$e\vec{v} \times \vec{B} = m\frac{v^2}{r} \qquad e\vec{B} = m\frac{v}{r}$$

$$v = \frac{1}{m}erB$$

By applying conservation of energy we derive an equation for charge mass ratio.

$$U_{\text{kin}} = \frac{1}{2}mv^2 \qquad U_{\text{pot}} = eV$$

$$\frac{1}{2}mv^2 = eV \qquad \frac{1}{2}m\left(\frac{1}{m}erB\right)^2 = eV$$

$$\frac{1}{2}\frac{1}{m}e^2r^2B^2 = eV \qquad \frac{1}{2m}er^2B^2 = V$$

$$\frac{e}{m} = \frac{2V}{r^2B^2}$$

Finally, we put the pieces together to derive an expression for current.

$$B^2 = 2mV\frac{1}{er^2} \qquad B = \sqrt{\frac{2mV}{er^2}} \qquad B = CI$$

$$\frac{2mV}{er^2} = C^2I^2$$

$$I^2 = \frac{2mV}{er^2C^2}$$

$$I = \left(\frac{1}{C}\sqrt{\frac{2mV}{e}}\right)\frac{1}{r}$$

Fig. 2: Current as a function of r

Now, we see a clear relationship between quantities we can measure and charge mass ratio.

Our experimental setup includes an apparatus with Helmholtz coils, a cathode ray, and measuring rod.

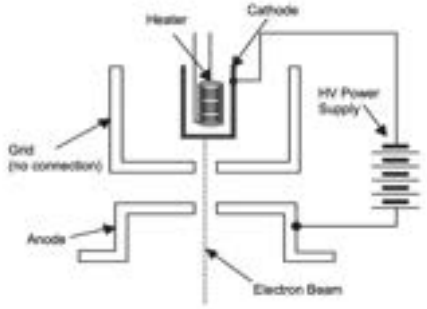

Fig. 3: Experimental Setup Diagram

Fig. 4: Experimental Setup

Firstly, we orient the apparatus so the Helmholtz coil so that their axes are parallel to the horizontal direction of the ambient magnetic field using a compass. Then we turn on the set up and set the accelerating voltage to 200V. We adjust the current nob until the circular deflection hits a desired radius. We repeat this for 5 different radii and record the current and radius of each trial.

200V	
Radius (cm)	Current (A)
0.050	1.12
0.045	1.25
0.040	1.41
0.035	1.61
0.030	1.86

Tab. 1: Radius of circular deflection and coil current for accelerating voltage of 200V

We repeat this procedure for four other accelerating voltages.

100V	
Radius (cm)	Current (A)
0.035	1.00
0.0325	1.10
0.030	1.17
0.0275	1.25
0.025	1.38

Tab. 2: Radius of circular deflection and coil current for accelerating voltage of 100V

300V	
Radius (cm)	Current (A)
0.050	1.41
0.045	1.57
0.040	1.76
0.035	2.01
0.030	2.34

Tab. 3: Radius of circular deflection and coil current for accelerating voltage of 300V

400V	
Radius (cm)	Current (A)
0.050	1.63
0.045	1.81
0.040	2.04
0.035	2.34
0.030	2.71

Tab. 4: Radius of circular deflection and coil current for accelerating voltage of 400V

500V	
Radius (cm)	Current (A)
0.050	1.86
0.045	2.04
0.040	2.29
0.035	2.62
0.030	3.00

Tab. 5: Radius of circular deflection and coil current for accelerating voltage of 500V

3 Results, Analysis & Discussion

To find e/m using our derived equation we must first plot the current versus the reciprocal of the radius.

200V	
Current (A)	1/Radius (cm^{-1})
1.12	20.0
1.25	22.2
1.41	25.0
1.61	28.6
1.86	33.3

Tab. 6: Current and reciprocal radius for accelerating voltage of 200V

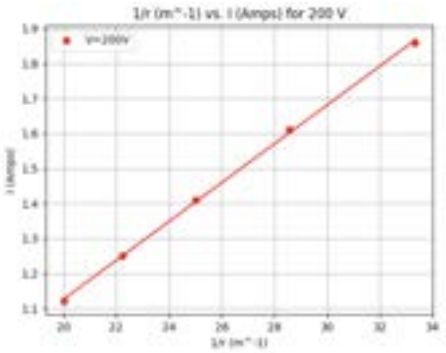

Fig. 5: Current versus 1/Radius for 200V

Given $I = A \cdot \frac{1}{r} + D$, we perform a weighted linear least squares fit to get a value for A and D as well as their uncertainties.

$$A = 0.056 \pm 0.00033$$
$$D = 0.016 \pm 0.00347$$

We repeat this for all setups.

Voltage (V)	A	σ_A	D	σ_D
100	0.032	7.1E-4	0.102	6.43E-3
200	0.056	3.3E-4	0.016	3.47E-3
300	0.070	1.0E-4	0.020	1.02E-3
400	0.081	3.2E-4	0.005	3.39E-3
500	0.086	6.3E-4	0.129	6.64E-3

Tab. 7: Linear Regression values and uncertainties

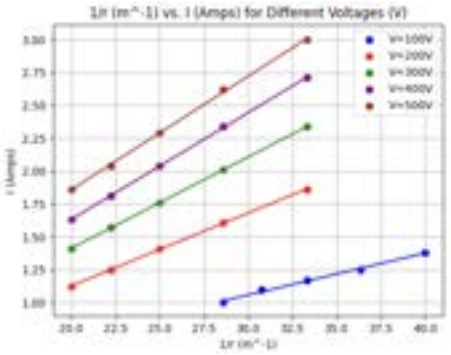

Fig. 6: Current versus 1/Radius for all Voltages

Let's recall the function we derived for I in terms of r.

$$I = \left(\frac{1}{C}\sqrt{\frac{2mV}{e}}\right)\frac{1}{r}$$

Combining our linear regression and the equation above we can use our slope or A to derive a value for e/m.

$$A = \frac{1}{C}\sqrt{\frac{2mV}{e}}$$

$$CA = \sqrt{\frac{2mV}{e}} \qquad C^2A^2 = \frac{2mV}{e} \qquad \frac{C^2A^2}{2V} = \frac{m}{e}$$

$$\frac{e}{m} = \frac{2V}{C^2A^2}$$

To complete this computation we must derive a value for our C constant.

$$B_I = \frac{\mu_0 R^2 N I}{(R^2 + (R/2)^2)^{3/2}} = (\frac{4\pi \times 10^{-7} N}{R(1+1/4)^{3/2}})I = C \times I$$

$$C = \frac{4\pi \times 10^{-7} N}{R(1+1/4)^{3/2}}, \quad N = 132, \quad R = .1475$$

$$C = .0008\, T A^{-1}$$

We calculate the following charge mass rations for five voltages. We propagate error by A and V to find the uncertainties.

Voltage (V)	e/m
100V	3.00E+11 ± 3.27E-2
200 V	1.97E+11 ± 3.65E+09
300 V	1.92E+11 ± 6.96E+08
400 V	1.87E+11 ± 2.34E+09
500 V	2.05E+11 ± 2.40E+09

Tab. 8: Calculated charge mass ratios for 5 voltages.

By weighting data points by error we find a weighted average and weighted standard error for charge mass ratio.

$$\overline{e/m} = 1.93 * 10^{11} \pm 6.32 * 10^{8}$$

4 Discussion

1. Our resulting weighted mean for charge mass ratio of $1.93 * 10^{11} \pm 6.32 * 10^{8}$ C kg^{-1} does statistically differ from the accepted value of 1.758×10^{11} C kg^{-1}. This could be due to several factors, including incorrectly reading the diameter for the current studied and not properly aligning the device resulting in an external magnetic field impacting our results.

2. One example of a systematic error that could be affecting our results is the impact of the external magnetic field. While we did our best to align our apparatus with the compass, we found some compasses to be faulty and it was difficult to precisely align the apparatus with the compass needle. A slight difference in angle could have skewed our results. Adjusting the nob to measure a precise radius and determining when the circular deflection matched the radius were difficult to do with precision. As a result, our recorded radii and currents are somewhat off affecting our final result for charge mass ratio.

3. For smaller radii, the circular beam become more hazy making it more difficult to take precise measurements. This means that measurements for current were more precise for larger r.

4. The expected value for D (the y-intercept of our 1/r versus current linear regression) should be 0, as when there is a radius of 0, the current should be zero. Our values for D agree within uncertainties to 0.

5 Conclusion

In this experiment we calculated a value for charge mass ration of $1.93 * 10^{11} \pm 6.32 * 10^{8}$ C kg^{-1}. Compared to the accepted value of 1.758×10^{11} C kg^{-1} our value does not fall within uncertainties. We note examples of systematic errors that could have resulted in this difference including skew from an external magnetic field and difficultly in obtaining precise measurements.

The discovery of the charge per mass ratio by JJ Thompson was a major breakthrough in the history of the atomic model. Today the principles of charge per mass of an electron are used in many applications including in mass spectrometers and particle accelerators.

6 Code

```
import matplotlib.pyplot as plt
import numpy as np
from scipy.stats import linregress

# Generate some sample data for demonstration
v1 = np.array([28.571, 30.769, 33.333, 36.363, 40.000])  # x values, 100
i1 = np.array([1.0, 1.1, 1.17, 1.25, 1.38])  # y values

v2 = np.array([20.000, 22.222, 25.000, 28.571, 33.333])  # x values, 200
i2 = np.array([1.12, 1.25, 1.41, 1.61, 1.86])  # y values

v3 = np.array([20.000, 22.222, 25.000, 28.571, 33.333])# x values, 300
i3 = np.array([1.41, 1.57, 1.76, 2.01, 2.34])  # y values

v4 = np.array([20.000, 22.222, 25.000, 28.571, 33.333])# x values, 400
i4 = np.array([1.63, 1.81, 2.04, 2.34, 2.71])  # y values

v5 = np.array([20.000, 22.222, 25.000, 28.571, 33.333])# x values, 500
i5= np.array([1.86, 2.04, 2.29, 2.62, 3])  # y values

x_error = np.array([.0025, .0025, .0025, .0025, .0025])
y_error = np.array([.005, .005, .005, .005, .005])

# Create a scatterplot for the first line
plt.scatter(v1, i1, label='V=100V', color='blue')
plt.scatter(v2, i2, label='V=200V', color='red')
plt.scatter(v3, i3, label='V=300V', color='green')
plt.scatter(v4, i4, label='V=400V', color='purple')
plt.scatter(v5, i5, label='V=500V', color='brown')

slope1, intercept1 = np.polyfit(v1, i1, 1)
fit_line1 = slope1 * v1 + intercept1
#plt.plot(v1, fit_line1, color='blue')
plt.errorbar(v1, fit_line1, xerr=x_error, yerr=y_error, color='blue')

slope2, intercept2 = np.polyfit(v2, i2, 1)
fit_line2 = slope2 * v2 + intercept2
#plt.plot(v2, fit_line2, color='red')
plt.errorbar(v2, fit_line2, xerr=x_error, yerr=y_error, color='red')

slope3, intercept3 = np.polyfit(v3, i3, 1)
fit_line3 = slope3 * v3 + intercept3
#plt.plot(v3, fit_line3, color='green')
plt.errorbar(v3, fit_line3, xerr=x_error, yerr=y_error, color='green')

slope4, intercept4 = np.polyfit(v4, i4, 1)
fit_line4 = slope4 * v4 + intercept4
#plt.plot(v4, fit_line4, color='purple')
plt.errorbar(v4, fit_line4, xerr=x_error, yerr=y_error, color='purple')

slope5, intercept5 = np.polyfit(v5, i5, 1)
fit_line5 = slope5 * v5 + intercept5
#plt.plot(v5, fit_line5, color='brown')
plt.errorbar(v5, fit_line5, xerr=x_error, yerr=y_error, color='brown')
```

```
# Add labels, legend, and title
plt.xlabel('1/r (m^-1)')
plt.ylabel('I (Amps)')
plt.legend()
plt.title('1/r (m^-1) vs. I (Amps) for Different Voltages (V)')

# Perform linear regression analysis for Line 4 A
slope1, intercept1, r_value1, p_value1, std_err1 = linregress(v1, i1)

# Perform linear regression analysis for Line 3.5 A
slope2, intercept2, r_value2, p_value2, std_err2 = linregress(v2, i2)

# Perform linear regression analysis for Line 3 A
slope3, intercept3, r_value3, p_value3, std_err3 = linregress(v3, i3)

# Perform linear regression analysis for Line 2.5 A
slope4, intercept4, r_value4, p_value4, std_err4 = linregress(v4, i4)

# Perform linear regression analysis for Line 2 A
slope5, intercept5, r_value5, p_value5, std_err5 = linregress(v5, i5)

# Calculate the errors for the slopes
slope_error1 = std_err1 / np.sqrt(5)
slope_error2 = std_err2 / np.sqrt(5)
slope_error3 = std_err3 / np.sqrt(5)
slope_error4 = std_err4 / np.sqrt(5)
slope_error5 = std_err5 / np.sqrt(5)

# calculate the errors for the y-int
residuals1 = i1 - slope1*v1 + intercept1
std_err_y_intercept1 = np.std(residuals1) / np.sqrt(3)

residuals2 = i2 - slope2*v2 + intercept2
std_err_y_intercept2 = np.std(residuals2) / np.sqrt(3)

residuals3 = i3 - slope3*v3 + intercept3
std_err_y_intercept3 = np.std(residuals3) / np.sqrt(3)

residuals4 = i4 - slope4*v4 + intercept4
std_err_y_intercept4 = np.std(residuals4) / np.sqrt(3)

residuals5 = i5 - slope5*v5 + intercept5
std_err_y_intercept5 = np.std(residuals5) / np.sqrt(3)

# Print
print(f"100V: Slope = {slope1:.3f} ± {slope_error1:.5f}")
print(f"100V: Intercept = {intercept1:.3f} ± {std_err_y_intercept1:.5f}")
print(f"200V: Slope = {slope2:.3f} ± {slope_error2:.5f}")
print(f"200V: Intercept = {intercept2:.3f} ± {std_err_y_intercept2:.5f}")
print(f"300V: Slope = {slope3:.3f} ± {slope_error3:.5f}")
print(f"300V: Intercept = {intercept3:.3f} ± {std_err_y_intercept3:.5f}")
print(f"400V: Slope = {slope4:.3f} ± {slope_error4:.5f}")
print(f"400V: Intercept = {intercept4:.3f} ± {std_err_y_intercept4:.5f}")
print(f"500V: Slope = {slope5:.3f} ± {slope_error5:.5f}")
print(f"500V: Intercept = {intercept5:.3f} ± {std_err_y_intercept5:.5f}")
```

```
# Show the plot
plt.grid(True)
plt.show()
```

Polarization and Inference (Revised Oct 2023)

Author: Tiffany Fu / Lab Members: Anvita Bansal, Alexandria Lam

1 Introduction

In this lab we explore two basic concepts of wave mechanics – polarization and inference – through a two part experiment with light.

Polarization occurs in transverse waves. In our lab we use a laser, which emits polarized light. We then use a polarization filter and analyzer to recreate the physics of two successive polarizers. We know that the intensity of light is proportional to the strength of the electric field squared. Additionally, we observe that the intensity of light after passing a polarization filter shifts and can be described by Malus' Law.

$$I = I_0 cos^2\theta$$

Fig. 1: Malus' Law

The second key property of waves is their ability to superimpose. Interference is the combination of two or more waves into a third wave. Thomas Young's Double Slit Experiment conducted in 1801 clearly demonstrated this wavelike property of light. Young passed a collimated light beam through two narrow slits and observed a wavelike interference pattern of the beam. He concluded that the bright and dark spots of the pattern were due to constructive and destructive interference. Using wave equations, we can use the double slit experiment to find the wavelength of light.

$$x_m = \left(\frac{\lambda D}{d}\right) m$$

Fig. 2: The Position of the mth maximum as a linear function of m

2 Method

In Part 1 we place a polarization analyzer with a rotary motion sensor (RMS) between a laser and light sensor. We push all components together to result in the following setup.

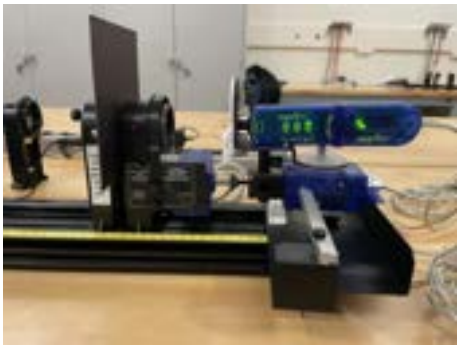

Fig. 3: Part 1 Experimental Setup Diagram

We begin by opening the "Polarization" file in DataStudio where we will be collecting data. We press start and slowly rotate the polarizer through one revolution. We record 20 data points of intensity and the corresponding angular position from the displayed graph.

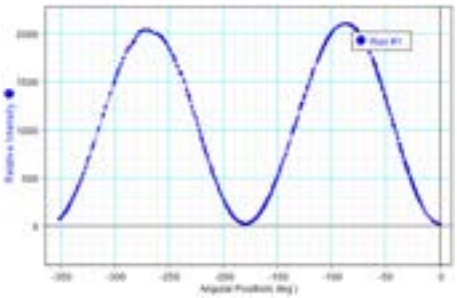

Fig. 4: Intensity vs. Angular Position Graph

Angular Position (rad)	Intensity
-6.11	74.45
-5.90	295.86
-5.71	605.69
...	...
-2.42	861.2
-2.17	1356.42
-1.88	1840.94
-1.53	2100.56
-1.12	1799.05
-0.79	1149.73
-0.46	481.58
-0.01	18.73

Tab. 1: Some Recorded Angular Position and Intensity Points

We record maximum intensity (I_0) and the corresponding angular position (θ_0)to be 2100.56 and -1.53 radians.

In Part 2 of our lab we will observe a double slit diffraction pattern. We remove the polarization analyzer from part one and place a double slit disk in front of the laser. We push the laser to the end of our track and measure a distance of 101 meters between the tip of the laser to the front of the light sensor.

Fig. 5: Part 2 Double Slit Experimental Setup

After initial set up we open "Interference" in DataStudio and click Start. We then slowly move the

Light Sensor across the translator arm to scan the full double slit pattern. Finally we record positions of the inference patterns maxima using SmartTools.

Position	Intensity
-0.088	0.16
-0.085	0.25
-0.082	0.34
...	...
-0.067	1.56
-0.064	2.91
-0.062	4.39
-0.059	5.59
-0.056	6.20
-0.054	5.78
-0.051	4.74
...	...
-0.030	0.40
-0.028	0.31
-0.025	0.19

Tab. 2: Some Recorded Maxima Points of Double Slit Diffraction Pattern

Next, we create a single slit envelope by adjusting a piece of cardboard to cover one of the slits on the double slit disk. We repeat the process of moving the light sensor across the pattern and record the data on DataStudio. Then we record the positions of the maxima of the single slit pattern. Lastly, we observe the following figure when overlapping curves from double slit diffraction and single slit envelope.

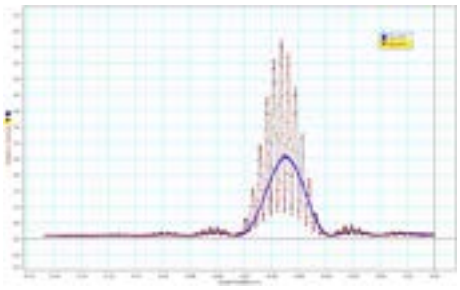

Fig. 6: Overlapping Experimental Curves of Double Slit Diffraction and Single Slit Envelope

3 Results, Analysis & Discussion

To test Malus' Law we will plot I/I_0 against $cos^2\theta$. Through data manipulation we arve at the following data points and scatter plot.

$cos^2\theta$	I/I_0
0.017	0.035
0.115	0.141
0.264	0.288
0.580	0.587
0.870	0.864
0.997	0.970
...	...

Tab. 3: Some I/I_0 versus $cos^2\theta$ Data Points

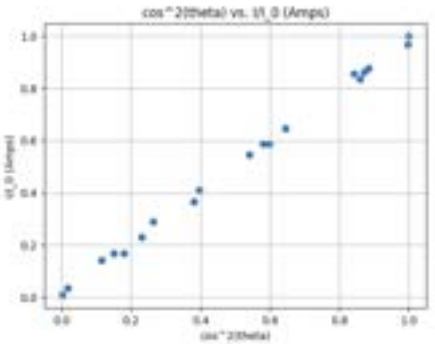

Fig. 7: I/I_0 versus $cos^2\theta$ Scatterplot.

We note that our scatter plot seems to follow a linear regression. This makes sense due to Malus' Law which states that the two variables are proportional. Considering this we perform a linear regression analysis to obtain a slope and intercept of 0.976 ± 0.00193 and 0.013 ± 0.00286.

When the polarizer is set at an angle of 90 degrees we read an intensity of 16.95. This is the noise of our light sensor. If there was no noise, we expect this value to be 0 since at 90 degrees all light should be absorbed by the filter.

The signal to noise ratio is equal to 2100.56 divided by 16.95. Our resulting ratio is 123.92. This tells us that the magnitude of our noise is small compared to our measured maximum intensity. This also shows the large range of intensity measured.

To reduce the potential influence of background light it would be more effective to change the setting of the experiment. Changing our data analysis could lead to bias or inaccurate results.

Noise arises from natural variances in machines. It would not be possible to completely remove it since perfect instruments are difficult to construct. Additionally if the analyzer was not perfectly perpendicular to the light not all light may have been absorbed leading to noise in the sensor.

We obtained a value of 0.013 ± 0.00286 for our y-intercept. This is statistically different than zero and is likely due to systemic errors such as a slightly tilted analyzer. The physical meaning of the y-intercept is when the polarizer is at θ_0, there is total interference and no light will pass through leading to a final intensity of zero.

If we performed the same experiment with an incandescent light we would yield different results since light produced by incandescent light bulbs are typically unpolarized. A polarization filter would be needed to be able to use the polarization analyzer. If there was no filter, the unpolarized light will emit light oscillating in random directions and no clear pattern would emerge in our graph.

Now we will move on with analyzing our double diffraction data. First we plot positions of maxima x_m against order number m.

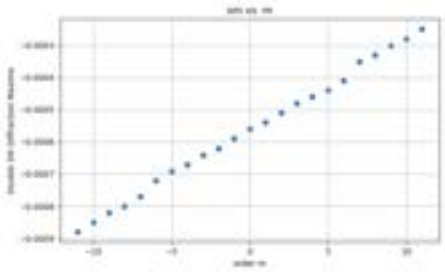

Fig. 8: Double Slit Diffraction Position Maxima versus Order Number

Next, we perform a least squares analysis to obtain a slope of $2.8 * 10^{-5} \pm 1 * 10^{-5}$ and intercept of -0.0056 $\pm$ 0.00002.

Let's recall our equation relating m and x_m.

$$x_m = \left(\frac{\lambda D}{d}\right) m$$

Fig. 9: Position of Maxima in terms of order number

With a distance D from slits to linear translator of 101 centimeters and a slit separation d of 0.25 millimeters, we can calculate wavelength using slope. We calculate a wavelength of 693 nanometers. The wavelength of the laser recorded was 650 nanometers so our calculated and expected values are similar.

In our double slit experiment we could see 23 fringes. The remaining fringes were not bright enough to be able to detect. If we increased the intensity of the laser we could have seen more fringes in our experiment.

The uncertainties in our measuring tools limits the precision of our measurement.

The slits to sensor distance would affect our data points. Changing the slit-to-light sensor spacing would change the slope of our graph.

For our single slit trial we will similarly plot the maxima positions(x_n) against order number n.

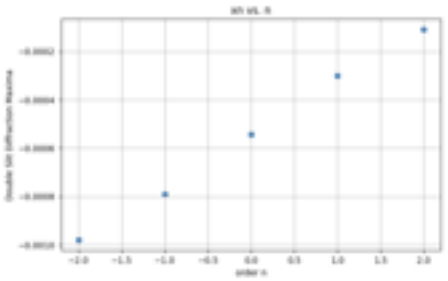

Fig. 10: Single Slit Diffraction Position Maxima versus Order Number

The slope of this plot is 0.000223.

$$x_n = \left(\frac{\lambda D}{a}\right) n$$

Fig. 11: Single Slit Diffraction Position Maxima versus Order Number

Using this equation, our slope, and the wavelength we calculated previously we derive an a value of 0.0314 millimeters. This value agrees with our nominal width of 0.04 mm.

Our double slit envelope is approximately twice as big as our single slit envelope. This means the sizes of the slit width and slit separation are relatively similar. This makes sense because we used the same slit setting for both trials. If we were to increase the slit width of the double-slit experiment, the double-slit envelope would be greater than double the size of the single-slit envelope since more light will pass through the slits leading to higher maximum intensity.

4 Conclusion

Through two separate experiments with light we observed two fundamental properties of waves: polarization and interference. In Part 1 by using a laser and polarization analyzer, we observe the shift in intensity as we rotate the polarized through one revolution. Through data analysis, we prove Malus' Law. We find noise in our sensor and note how a tilted analyzer may be a systemic error causing this noise. In Part 2, we recreate a double-slit experiment and use a light sensor to trace the diffraction pattern. We also cover one slit and repeat the process to get a single-slit envelope. By plotting maxima against order numbers for both trials we use gathered slopes and equations to predict properties including wavelength and slit width. We compare these to their recorded values. Finally, we note that out double-slit envelope is roughly double the size of our single-slit envelope.

Light and many other physical properties are composed of waved. Through performing this lab we begin to understand the basic mechanics and interactions of waves.

5 Code

```
import matplotlib.pyplot as plt
import numpy as np
from scipy.stats import linregress

cossquare = np.array([0.01749175276, 0.1147433786, 0.2637246176, 0.5799405938, 0.8704022981, 0.9968839596,
x_error = np.full(21, .1)

ioverizero = np.array([0.0354429295, 0.1408481548, 0.288346917, 0.5872434018, 0.8635221084, 0.9698128118,
y_error = np.full(21, 1)

plt.scatter(cossquare, ioverizero)

mean_x = np.mean(cossquare)
mean_y = np.mean(ioverizero)

n = len(cossquare)  # Number of data points

numerator = np.dot(cossquare - mean_x, ioverizero - mean_y)
denominator = np.dot(cossquare - mean_x, cossquare - mean_x)

slope = numerator / denominator
intercept = mean_y - slope * mean_x

y_pred = slope * cossquare + intercept

# plt.plot(cossquare, y_pred)
#plt.errorbar(cossquare, y_pred, yerr=y_error, xerr=x_error)

plt.xlabel('cos^2(theta)')
plt.ylabel('I/I_0 (Amps)')
plt.title('cos^2(theta) vs. I/I_0 (Amps)')

# print(f"Slope (Coefficient): {slope:.2f}")
# print(f"Intercept: {intercept:.2f}")

slope1, intercept1, r_value1, p_value1, std_err1 = linregress(cossquare, ioverizero)

slope_error1 = std_err1 / np.sqrt(n)

residuals1 = ioverizero - slope1*cossquare + intercept1
std_err_y_intercept1 = np.std(residuals1) / np.sqrt(n-1)

print(f"Slope = {slope:.3f} ± {slope_error1:.5f}")
print(f"Intercept = {intercept:.3f} ± {std_err_y_intercept1:.5f}")

plt.grid(True)
plt.show()

order = np.array([-11, -10, -9, -8, -7, -6, -5, -4, -3, -2, -1, 0, 1, 2, 3, 4, 5, 6, 7, 8, 9, 10, 11])

position = np.array([-0.00088, -0.00085, -0.00082, -0.0008, -0.00077, -0.00072, -0.00069, -0.00067, -0.000

mean_x = np.mean(order)
mean_y = np.mean(position)
```

```
numerator = np.dot(order - mean_x, position - mean_y)
denominator = np.dot(order - mean_x, order - mean_x)

slope = numerator / denominator
intercept = mean_y - slope * mean_x

slope1, intercept1, r_value1, p_value1, std_err1 = linregress(order, position)

slope_error1 = std_err1 / np.sqrt(len(order))

residuals1 = position - slope1*order + intercept1
std_err_y_intercept1 = np.std(residuals1) / np.sqrt(len(order)-1)

plt.xlabel('order m')
plt.ylabel('Double Slit Diffraction Maxima')
plt.title('xm vs. m')

print(f"Slope = {slope:.6f} ± {slope_error1:.5f}")
print(f"Intercept = {intercept:.3f} ± {std_err_y_intercept1:.5f}")

plt.scatter(order, position)

plt.grid(True)
plt.show()

ordern = np.array([-2, -1, 0, 1, 2])

positionn = np.array([-0.00098, -0.00079, -0.000543, -0.0003, -0.00011])

mean_x = np.mean(ordern)
mean_y = np.mean(positionn)

numerator = np.dot(ordern - mean_x, positionn - mean_y)
denominator = np.dot(ordern - mean_x, ordern - mean_x)

slope = numerator / denominator
intercept = mean_y - slope * mean_x

slope1, intercept1, r_value1, p_value1, std_err1 = linregress(ordern, positionn)

slope_error1 = std_err1 / np.sqrt(len(ordern))

residuals1 = positionn - slope1*ordern + intercept1
std_err_y_intercept1 = np.std(residuals1) / np.sqrt(len(ordern)-1)

plt.xlabel('order n')
plt.ylabel('Double Slit Diffraction Maxima')
plt.title('xn vs. n')

print(f"Slope = {slope:.6f} ± {slope_error1:.5f}")
print(f"Intercept = {intercept:.3f} ± {std_err_y_intercept1:.5f}")

plt.scatter(ordern, positionn)

plt.grid(True)
```

```
plt.show()
```

The Spectrum of the Hydrogen Atom (Revised Nov 2023)

Author: Tiffany Fu / Lab Members: Anvita Bansal, Alexandria Lam

1 Introduction

In furthering our studies of light and waves we turn to its interaction with chemistry, specifically atomic structures. In this experiment we observe the discrete light spectrum from a gas discharge lamp to map the spectrum of the hydrogen atom. An important equation we consider is Balmer's equation to predict the wavelengths of the visible lines of the spectrum.

$$\frac{1}{\lambda} = R\left(\frac{1}{n_f^2} - \frac{1}{n_i^2}\right)$$

Fig. 1: Balmer's Formula

To decompose a spectrum, one can use transmission grating where a grating is a slab of material with tiny parallel slits. The spacing between slits d is the "lattice constant" of the grating. Using interference formulas we can relate the lattice constant with positional maxima and wavelength of light passing through. This equation tells us that the maxima of a given wavelength will occur at different angles in relation to the laser beam.

$$d\sin\theta = m\lambda$$

Fig. 2: Formula relating maxima, wavelength, angle, and lattice energy

Using both these equations we can find the initial atomic shell number n_i in terms of $R, s, m, \text{and}\theta$ for a final atomic shell number of 2.

$$n_i = 2\sqrt{\frac{dR\sin\theta}{dR\sin\theta - 4m}}$$

Fig. 3: Formula for Initial Atomic Shell Number

2 Method

In this experiment we will use a diffraction grating spectrometer which is mainly composed of a collimator tube, a rotating table, and a telescope. We align our spectrometer to our light source – a helium lamp for part 1 and hydrogen lamp for part 2. We place the grating between and the telescope and collimator tube. The rotating table allows the telescope to swivel so we can observe the angle dependence of the various spectral lines.

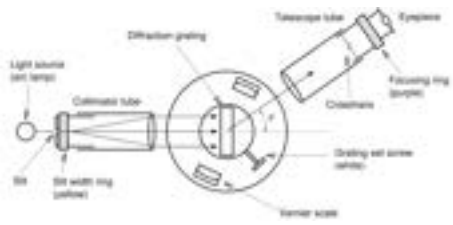

Fig. 4: Experimental Setup Diagram

We begin by obtaining our grating lattice component. After aligning our spectrometer, we turn a helium discharge lamp which emits light of wavelength $5.8756\ \times 10^{-7}$. We rotate the spectrometer leftwards until we observe a yellow beam. We record the angle of this observation and then find the location of the yellow beam by rotating the spectrometer right of the laser beam. We use the Vernier ruler to measure our angles to the nearest arcminute.

θ_L	θ_R	θ_A (rad)
$20°58'$	$20°53'$	0.36521

Tab. 1: Observed Leftside, Rightside, and Average Angle of Yellow Light emitted from Helium Lamp

We recall our grating equation and use $m = 1$ to determine the lattice constant.

$$d\sin\theta = m\lambda$$
$$d\sin(0.36521) = 5.8756 \times 10^{-7}$$
$$d = 1.6452 \times 10^{-6}$$

This corresponds to 607.85 lines mm^{-1}. We note that we could also see the second and third order yellow lines on both sides of $\theta = 0°$. If we also took these measurements we could improve the accuracy of our calculated value.

After obtaining our grating value we will now complete a similar experiment with a hydrogen lamp. When light from the hydrogen lamp is emitted through the spectrometer there are four visible lines on the spectrum – one red, one greenish-blue, one purple- blue and one dark purple. We measure the angles of these beams on both sides for two orders of the spectrum.

	θ_L	θ_R	$\bar{\theta}$ (rad)
Dark-purple	$14°33'$	$14°28'$	0.2532
Purple	$15°21'$	$15°15'$	0.2670
Greenish-blue	$17°15'$	$17°6'$	0.2998
Red	$23°39'$	$23°25'$	0.4108

Tab. 2: Observed Leftside, Rightside, and Average Angles of First Order Beams of Hydrogen Spectrum

	θ_L	θ_R	$\bar{\theta}$ (rad)
Dark-purple	$30°14'$	N/A	0.5277
Purple	$32°11'$	$31°35'$	0.5565
Greenish-blue	$36°40'$	$35°54'$	0.6353
Red	$54°7'$	$52°0'$	0.9261

Tab. 3: Observed Leftside, Rightside, and Average Angles of Second Order Beams of Hydrogen Spectrum

We saw three orders. We observe that the second and third orders overlapped. This makes sense because according to the grating equation the ratio of the angle of second order to the maximum angle of the third order is greater than one.

3 Results & Analysis

With our resulting angles of diffraction we will begin by calculating the wavelengths of light using our grating equation for first-order (m=1) and second order (m=2) using our previously calculated grating constant.

$$d \sin \theta = m\lambda$$

	$\bar{\theta}$ (rad)	λ (nm)
Dark-purple	0.2532	412.12
Purple	0.2670	434.14
Greenish-blue	0.2998	485.86
Red	0.4108	656.91

Tab. 4: Average Angles and Calculated Wavelengths of First Order Beans of Hydrogen Spectrum

	$\bar{\theta}$ (rad)	λ (nm)
Dark-purple	0.5277	414.21
Purple	0.5565	434.47
Greenish-blue	0.6353	488.13
Red	0.9261	657.45

Tab. 5: Average Angles and Calculated Wavelengths of Second Order Beans of Hydrogen Spectrum

Next, we will apply Balmer's equation to calculate n_i for both orders with $R = 1.0974 \times 10^7 \mathrm{m}^{-1}$ and $n_f = 2$.

	λ (nm)	n_i
Dark-purple	412.12	5.8837
Purple	434.14	4.9937
Greenish-blue	485.86	4.0017
Red	656.91	2.9977

Tab. 6: Calculated Wavelengths and Initial Atomic Shell Number of First Order Beans of Hydrogen Spectrum

	λ (nm)	n_i
Dark-purple	414.21	5.7732
Purple	434.47	4.9838
Greenish-blue	488.13	3.9740
Red	657.45	2.9962

Tab. 7: Calculated Wavelengths and Initial Atomic Shell Number of Second Order Beans of Hydrogen Spectrum

4 Discussion

1. Our results for n_i are very close to integers and are consistent with the predictions of the Balmer Formula and the Bohr Model. Both were fairly accurate but the first order beams yielded results that were closer to integers.
2. The electrons of the red beam jumped from the lowest shell number ($n_i = 2$). This can be predicted as we know that red light has the longest wavelength on the visible spectrum. This means that according to Balmer's equation n_i will need to be the smallest integer to yield the smallest result for $(\frac{1}{n_f^2} - \frac{1}{n_i^2})$ which is proportional to the reciprocal of the wavelength.
3. The energy differences of shells correspond to the difference in energy of electrons jumping from the initial shell to the final shell of 2. The following diagram displays energy differences for a hydrogen atom[1]. We see that the gaps in energy difference decreases as the final shell number increases. The electrons of He/H get excited by the high voltage passed through the lamps.

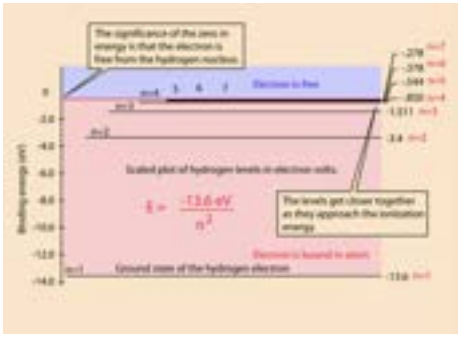

Fig. 5: Energy Differences Diagram

4. We had the most precise measurements for the red light of initial energy level 2.
5. We can only see four lines in the hydrogen spectrum because the human eye can only detect light with wavelengths between 400 and 700nm. From our calculations we see that the wavelengths of the four lines fall within this range. The other emission lines are possibly too short or too long to be detected with the human eye.
6. The zeroth order line is the beam we see when the spectrometer is directly pointed towards the lamp. This is the light that experiences no diffraction from the grating.
7. To observe how precise our results are, we will compare expected and actual values by calculating percent error.

Light	Percent Error
Dark-purple	1.9645
Purple	0.1121
Greenish-blue	-0.0611
Red	0.0747

Tab. 8: Percent Error

These percent errors are much lower than the results of our previous lab experiments. This is likely due to how accurately we were able to measure our data in this lab using the Vernier ruler.

8. The precision of measurements for wavelength is greater as compared to Polarization/Interference and Interferometer labs where our percent errors were significantly larger.

9. The thickness of spectral beams creates uncertainty in our measurements. This is a systematic error. Background light from nearby devices or light reflections are random factors that could also create uncertainty in our measurements.

5 Conclusion

In this experiment we observe the light spectrum of the hydrogen atom by using a diffraction grating spectrometer. We first obtain an accurate lattice constant d by measuring the diffraction angle of yellow light from a helium lamp. We conclude with a lattice constant of 1.6452×10^{-6} corresponding to 607.85 lines mm^{-1} on the grating.

Next, we observe the light spectrum of the hydrogen atom by using a hydrogen lamp. We measure the angles of four visible beams for two orders. In our data analysis, we calculate the wavelengths and initial atomic shell numbers of each light beam. Our results for this lab are significantly more accurate than previous labs. This is likely due to how precisely we were able to record our measurements using the Vernier ruler and the precision of the spectrometer

By observing the light spectrum of the hydrogen atom we further our understanding of atomic structure and how to observe energy differences in atomic particles. Through this lab we have elevated our understanding of the tight relationship between physics and chemistry.

6 Citations

1. Nave, R "Hyperphysics," GSU. 2023. http://hyperphysics.phyastr.gsu.edu/hbase/hyde.html

Capacitance and the Oscilloscope (Revised Nov 2023)

Author: Tiffany Fu / Lab Members: Anvita Bansal, Alexandria Lam

1 Introduction

Capacitors are one of the Big Three Passive Components – the trio of elements that form basic electronic circuits. Capacitors store electrical energy by distributing charged particles on multiple plates to create a potential difference. This powerful function makes the capacitor an extremely useful component. In fact, capacitors are a part of almost all electrical applications we use today. In this lab we closely observe the behavior of a capacitor as is charges and discharges. In a simple RC circuit (a circuit composed of a battery, resistor, and capacitor) the charging of a capacitor can be described with the following function.

$$I(t) = \frac{\varepsilon}{R} e^{-t/RC}$$

Fig. 1: RC Circuit Charging Current Equation as Function of Time

The predicted discharging behavior is similar to the charging process but opposite in signage. It can be described using the following equation.

$$I(t) = -\frac{\varepsilon}{R} e^{-t/RC}$$

Fig. 2: RC Circuit Discharging Current Equation as Function of Time

In the second part of this lab we explore the charging and discharging of a small RC combination using the oscilloscope. The oscilloscope is a powerful tool that is used to measure varying voltages and is composed of capacitors!

2 Method

Part 1

In order to observe the charging and later discharging of a capacitor we must set up a circuit, specifically an RC circuit. Our experimental setup is composed of a power supply, an ammeter, a switch, capacitors connected in parallel with three switches, and a resistor all connected with electrical wires. The following is our circuit diagram.

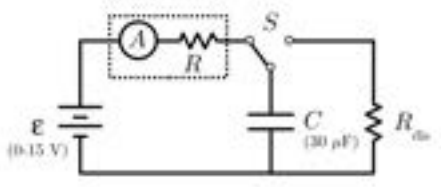

Fig. 3: Switch Circuit Setup for Observing Charging Capacitor

With a 15V Power Supply and 10 μF Capacitance we turn on the battery to charge the capacitor. We film a video of the ammeter and record the current displayed at 3 second intervals. We repeat this for a second trial and then for 20 μF and 30 μF Capacitance.

Seconds	Trial 1 (V)	Trial 2 (V)	Avg (V)
0	40.0.	40.0	40.0
3	17.3	17.8	17.55
6	12.5	10.6	11.55
9	7.6	11.5	9.55
12	4.7	4.1	4.40
15	2.8	2.5	2.65
18	1.7	1.6	1.65
21	1.1	1.1	1.10
24	0.9	0.8	0.85
27	0.5	0.6	0.55

Tab. 1: Recorded Charging Current through Ammeter with 10 μF Capacitance

Seconds	Trial 1 (V)	Trial 2 (V)	Avg (V)
0	39.0	41.5	40.25
3	22.0	23.5	22.75
6	12.1	17.7	14.90
9	13.1	13.6	13.35
12	10.1	10.5	10.30
...	...	...	...
33	1.9	1.9	1.90
36	1.5	1.5	1.50
39	1.2	1.2	1.20
42	1.1	1.0	1.05
45	1.0	0.8	0.90

Tab. 2: Recorded Charging Current through Ammeter with 20 μF Capacitance

Seconds	Trial 1 (V)	Trial 2 (V)	Avg (V)
0	40.0	41.7	40.85
3	24.0	25.6	24.80
6	20.6	20.7	20.65
9	12.5	18.2	15.35
12	14.5	15.2	14.85
...	...	...	...
54	1.5	1.5	1.50
57	1.2	1.3	1.25
60	1.1	1.1	1.10
63	1.0	1.0	1.00
66	1.0	0.9	0.95

Tab. 3: Recorded Charging Current through Ammeter with 30 μF Capacitance

We then move components around to the following circuit diagram so that the ammeter can be used to measure the discharging behavior.

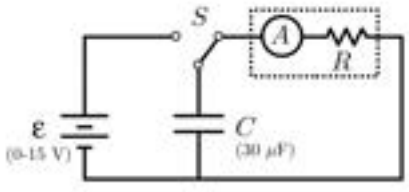

Fig. 4: Switch Circuit Setup for Observing Discharging Capacitor

Similarly we record the current through the wire during discharge at regular intervals for two trials at three different values of capacitance.

Seconds	Trial 1 (V)	Trial 2 (V)	Avg (V)
0	40.0	40.5	40.25
3	20.0	19.0	19.50
6	12.0	11.5	11.75
9	9.5	8.8	9.15
12	8.3	7.8	8.05
15	7.3	6.9	7.10
18	6.4	6.0	6.20
21	5.8	5.3	5.55
24	5.0	4.8	4.90
27	4.5	4.1	4.30

Tab. 4: Recorded Discharging Current through Ammeter with 10 μF Capacitance

Part 2

In the next part of our lab procedure we aim to observe an accurate value of the time constant of small RC combination using an oscilloscope. First, we reassemble our circuit to the following arrangement.

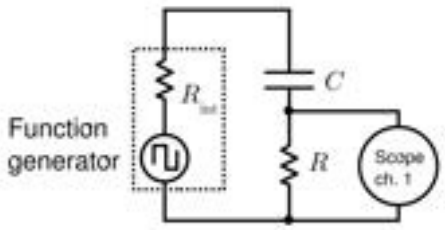

Fig. 5: Circuit Setup for Observing Small RC Combination

We know that after the time constant $\tau = RC$ the voltage will drop to $1/e = 37\%$ of its initial value. Using the multipurpose nob and cursor of the oscilloscope we read off the time difference between these initial voltage and thirty-seven percent of voltage. We repeat for another value of the function generator frequency and record the following results.

Frequency (Hz)	141.00	124.45
Voltage (V) (s)	5.12	5.12
Time Constant (μs)	780	820

Tab. 5: Frequency, Voltage, and Time Constant for Varied Frequency in RC Combination

The uncertainty of Voltage and Time are 0.08V and 10s due to the oscilloscope intervals.

3 Results & Analysis

We begin our data analysis by linearizing our exponential function for current.

$$I(t) = \tfrac{\varepsilon}{R} e^{-t/RC}$$
$$I = I_0 e^{-t/RC}$$
$$\ln I = \ln\left(I_0 e^{-t/RC}\right) = \ln I_0 - \left(\tfrac{1}{RC}\right) t$$

We record the natural log of our values for current and uncertainties and plot them against time to get a linear graph.

Seconds	I	$\ln(I)$
0	40.0	3.69
3	17.55	2.87
6	11.55	2.45
9	9.55	2.26
12	4.40	1.48
15	2.65	0.97
18	1.65	0.50
21	1.10	0.10
24	0.85	-0.16
27	0.55	-0.60

Tab. 6: Current and Natural Log of Current of Charging RC Circuit with 10 μF Capacitance

We calculate error using variance.

$$\sigma_I = \sqrt{\frac{\sum_{i=1}^{N}(I_i - \bar{I})^2}{N(N-1)}} = \frac{s}{\sqrt{N}}$$

For our first data set $\sigma_I = 1.50$ and $\sigma_{\ln I} = 0.00678$.

After manipulating our data we perform linear regressions to obtain the slopes and uncertainties for our three capacitances in a charging circuit.The slope translates to $1/RC$ where RC is time constant τ. We take the reciprocals of slope to obtain our time constant and then divide this value by capacitance to obtain a value for internal resistance R.

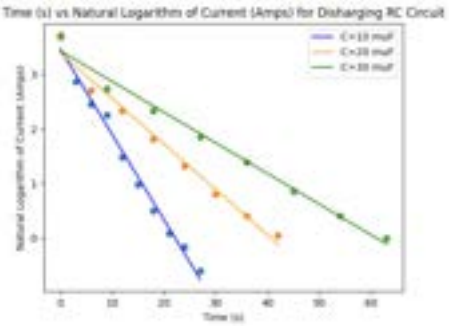

Fig. 6: Graph of Three Capacitances

Our uncertainties are calculated using the Standard Error of a Regression Slope formula.

$$s(b) = \sqrt{\frac{1}{n-2} * \frac{\sum(y_i - \hat{y})^2}{\sum(x_i - \bar{x})^2}}$$

Fig. 7: Standard Error of a Regression Slope

	Slope	$\tau(s)$	$R(\mathrm{M}\Omega)$
10 μF	-0.156 ± 0.0060	6.410	6.410
20 μF	-0.0808 ± 0.0044	12.376	6.188
30 μF	-0.0549 ± 0.0026	18.215	6.072

Tab. 7: Slope, Time Constant, and Resistance Values for Capacitances

Our final value for internal resistance is 6.223 ± 0.099MΩ where uncertainty is derived by variance. Finally, to check the accuracy of our results for τ we compare the ratios of τ for the different capacitances.

$$\tau_{30\mu F}/\tau_{20\mu F} = 1.472$$

$$\tau_{30\mu F}/\tau_{10\mu F} = 2.84$$

$$\tau_{20\mu F}/\tau_{10\mu F} = 1.93$$

We note that our ratios are all close to the expected values and most agree within uncertainties.

4 Discussion

The measurements of from the digital scope indicate an experimental value of 800s, while the expected value of τ using C = 83 nF and R = 10,050 Ω is 834s.

Circuit elements with poor tolerance would result in uncounted resistance and impedance in the circuit altering our results for τ and explaining discrepancies in our values.

The shape of our voltage graph follows an exponential decay curve which is as expected by our function for current through a charging capacitor. The voltage provided by the function generator of the oscilloscope has an amplitude of 10V. This mean that the average voltage provided is 5V and our value of 5.12V agrees with what was expected.

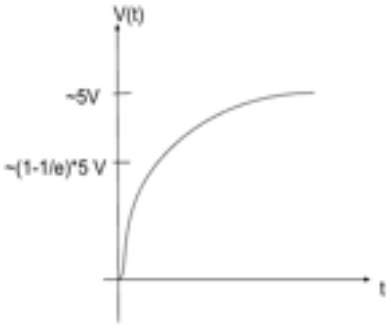

Fig. 8: Voltage Difference Across a Capacitor

The voltage across the resistor and capacitor should have similar shapes but opposite in concavity. The total voltage of both elements must add up to the original voltage due to Kirchoff's Loop Law.

Since the internal resistance and resistor are placed in parallel including the approximate internal resistance of the scope as 1MΩ would not vastly change the behavior or voltage. On the other hand using a 1MΩ resistor in place of the 10kΩ resistor would increase the time constant by 100s.

Completing the experiment with a higher frequency such as 1kHz would shrink the graph displayed by the oscilloscope and make it more difficult to determine the time constant. Accurate measurements of can be best recorded from approximately 100Hz to 1200Hz, the frequency where f=$\frac{1}{\tau}$.

5 Conclusion

In this experiment we observed the charging and discharging behavior of both a small RC and large RC. By recording current data through an ammeter at regular intervals and linearizing our current equation we can perform a linear regression. Through analysis we yield time constants of $\tau_{10\mu F} = 6.41$, $\tau_{20\mu F} = 12.38$,and $\tau_{30\mu F} = 18.22$ as well as a value of $6.223 \pm 0.099\mathrm{M}\Omega$ for internal resistance.

In part two of this lab we use an oscilloscope to observe voltage and time constants under varying frequencies. Our digital scope resulted in an experimental time constant of 800s which is similar to the expected value of 834s. We note systematic errors such as low tolerance and unaccounted resistance in circuit wires as factors of discrepancy.

This lab introduced us to the oscilloscopes, an important tool used in engineering to measure electrical phenomena and quickly debug circuits. Outside of experimental studies, oscilloscopes are used in automotive tests, signal analyses, and power measurements.

6 Code

```
import matplotlib.pyplot as plt
import numpy as np
import pandas as pd
from scipy.stats import linregress

# C = 10
df = pd.read_csv('c10d1.csv')

x1 = np.array(df['Time'])
y1 = np.array(df['LnCurrent'])
error1 = np.array(df['LnCurrentError'])

# C = 20
df = pd.read_csv('c20d1.csv')

x2 = np.array(df['Time'][::2])
y2 = np.array(df['LnCurrent'][::2])
error2 = np.array(df['LnCurrentError'][::2])

# C = 30
df = pd.read_csv('c30d1.csv')

x3 = np.array(df['Time'][::3])
y3 = np.array(df['LnCurrent'][::3])
error3 = np.array(df['LnCurrentError'][::3])

# Scatter plot
plt.scatter(x1, y1)
# plt.errorbar(x1, y1, yerr=error1, fmt='none')

# Linear regression
slope1, intercept1, r_value1, p_value1, std_err1 = linregress(x1, y1)
line1 = slope1 * x1 + intercept1

# Plot the regression line
plt.plot(x1, line1, color='blue', label='C=10 muF')

# Scatter plot
plt.scatter(x2, y2)
# plt.errorbar(x2, y2, yerr=error2, fmt='none')

# Linear regression
slope2, intercept2, r_value2, p_value2, std_err2 = linregress(x2, y2)
line2 = slope2 * x2 + intercept2

# Plot the regression line
plt.plot(x2, line2, color='orange', label='C=20 muF')

# Scatter plot
plt.scatter(x3, y3)
# plt.errorbar(x3, y3, yerr=error3, fmt='none')

# Linear regression
slope3, intercept3, r_value3, p_value3, std_err3 = linregress(x3, y3)
```

```
line3 = slope3 * x3 + intercept3

# Plot the regression line
plt.plot(x3, line3, color='green', label='C=30 muF')

# Adding labels and title
plt.xlabel('Time (s)')
plt.ylabel('Natural Logarithm of Current (Amps)')
plt.title('Time (s) vs Natural Logarithm of Current (Amps) for Disharging RC Circuit')
# plt.title('Time (s) vs Natural Logarithm of Current (Amps) when C = 10 muF')
plt.legend()

# Display linear regression statistics
print(f"Slope: {slope1:.3f}")
print(f"Intercept: {intercept1:.3f}")
print(f"R-squared value: {r_value1**2:.2f}")
print(f"Standard Error of Slope: {std_err1:.5f}")

print(f"Slope: {slope2:.3f}")
print(f"Intercept: {intercept2:.3f}")
print(f"R-squared value: {r_value2**2:.2f}")
print(f"Standard Error of Slope: {std_err2:.5f}")

print(f"Slope: {slope3:.3f}")
print(f"Intercept: {intercept3:.3f}")
print(f"R-squared value: {r_value3**2:.2f}")
print(f"Standard Error of Slope: {std_err3:.5f}")

# Show the plot
plt.show()
```

AC Circuits (Revised Dec 2023)

Author: Tiffany Fu / Lab Members: Anvita Bansal, Alexandria Lam

1 Introduction

Following last weeks reports on RC Circuits we continue the investigation of electrical circuits with a focus on AC Circuits in this lab. AC Circuits are circuits which contain the usual elements of resistors, capacitors, inductors, etc. but are driven by a voltage that varies in time.

In our experiment we setup a RLC Circuit. For a sinusoidal time-dependent voltage $V(t)$ we use Kirchoff's Loop Rule and find that the current in each element will be sinusoidal.

$$\sum \Delta V = 0 = V(t) - V_R - V_L - V_C$$
$$V(t) = IR + L\frac{dI}{dt} + \frac{q}{C} = IR + \frac{dI}{dt} + \frac{1}{C}\int Idt$$
$$V(t) = V_{\max}\sin\omega t + \phi_V$$
$$I(t) = I_{\max}\sin\omega t + \phi_I$$

Using Ohm's Law and Faraday's Law, we first derive the isolated voltage in the resistor, inductor, and capacitor.

$$V_R = I(t) * R = I_{\max}R\sin\omega t$$
$$V_L = \omega L I_{\max} cos\omega t$$
$$V_C = \frac{1}{C}\left(\frac{-I_{\max}}{\omega}cos\omega t\right)$$

By replacing variables with a reactance quantity (X), we can represent the maximum voltage in the inductor and capacitor.

$$V_{\max} = I_{\max}X_L \ , \ X_L = \omega L$$
$$V_{\max} = I_{\max}X_C \ , \ X_C = \frac{1}{\omega C}$$

Combining our results we can find the maximum voltage of the RLC combination where Z is the impedance of the RLC circuit.

$$V_{\max} = I_{\max}Z \ , \ Z = \sqrt{R^2 + (X_L - X_C)^2}$$

The resistive part of Z (just the resistor) resists all voltage supply as heat with the reactive part of Z (the combination of the inductance and capactior does not dissipate energy. Resonance describes when the impedance takes on a minimum value $(X_L = X_C)$ and driving voltage is at a maximum. The resonance frequency is $\frac{1}{\sqrt{LC}}$.

2 Method

Part 1: Resonance

Our experimental setup once again includes the oscilloscope along with a decade resistor box, a capacitor, two inductors, and a function generate. We arrange the elements to correspond with the following diagram.

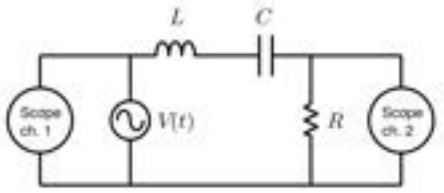

Fig. 1: Experimental Setup of RLC Circuit, Function Generator, and Oscilloscope

We first set up the function generator to a signal in the range of 1 kHz and a peak-to-peak voltage of 20 V. We set the decade resistor box to a resistance of 50 Ω. Using the frequency node on the function generate we sweep through until we observe a maximum in the pea-to-peak voltage. After we find the resonance frequency we scan over surrounding frequencies and record their peak-to-peak voltages.

Voltage (V)	Frequency (Hz)
1.92	596
1.78	496
1.84	505
1.9	616
1.82	560
...	...
1.48	950
1.52	860
1.28	298
1.82	463
1.18	287
1.04	250

Tab. 1: Voltage and Frequency of RLC Circuit with 50 Ω Resistance

We repeat this for a resistance of 10 Ω and 500 Ω.

Voltage (mV)	Frequency (kHz)
160	22
120	29
110	18
138	34
146	16
...	...
132	41
124	12
120	52
116	11
121	30

Tab. 2: Voltage and Frequency of RLC Circuit with 10 Ω Resistance

Voltage (mV)	Frequency (kHz)
11.2	558
10.8	529
10.4	414
10	343
9.2	317
...	...
8.8	1136
8.4	1235
8	1316
7.6	1515
7.2	1639

Tab. 3: Voltage and Frequency of RLC Circuit with 500 Ω Resistance

Next, we replace the 150 mH inductor with a large copper ring of unknown inductance. We once again sweep through the range of frequencies until we find a resonance frequency of 4170 Hz. 2.91 mH.

Part 2: Phase of $V(t)$, V_L, and V_C

In the next part we observe phase shifts. We replace the copper ring with the original 150 mH inductor and set the resistance to 30 ω. We record the time for one full cycle of the driving signal T_d and then measure the time difference $t_R - t_d$ for five values of frequency around the resonance frequency ω_0. We calculate the phase difference ϕ with the following formula.

$$\phi = 2\pi \frac{t_R - t_d}{T_d}$$

Fig. 2: Phase Difference Equation

f (Hz)	T_d (s)	$t_R - t_d$ (s)	ϕ (rad)	σ_ϕ
481	0.0021	-0.0001	-0.395	0.021
530	0.0019	-0.0007	-2.339	0.024
581	0.0017	0.0000	0.000	0.000
630	0.0016	0.0006	2.356	0.029
681	0.0015	0.0001	0.427	0.030

Tab. 4: Experimental Driving Phase Differences of Resistor

We repeat this process to observe the phase differences of the inductor and capacitor.

f (Hz)	T_d (s)	$t_R - t_d$ (s)	ϕ (rad)	σ_ϕ
4450	0.00042	0.00008	1.197	0.107

Tab. 5: Experimental Driving Phase Differences of Inductor

f (Hz)	T_d (s)	$t_R - t_d$ (s)	ϕ (rad)	σ_ϕ
50	0.0186	0.0048	1.621	0.002

Tab. 6: Experimental Driving Phase Differences of Capacitor

3 Results, Analysis & Discussion

Part 1

1. We begin our data analysis by plotting our three sets of peak-to-peak voltages as a function of frequency. We normalize each to the maximum and conclude with the following figure.

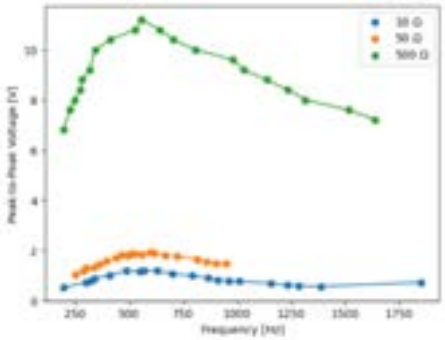

Fig. 3: Peak-to-Peak Voltages vs. Resonance Frequency for Three Resistances

2. The resonance frequency ω of our RLC circuit was 581.2 ± 0.64.

3. Using our equation for resonance frequency and an inductance of 150 mH and capacitance of 0.5 μF our expected value for resonance is 581.15 s. Our expected and experimental frequencies do agree within error

4. We calculated an inductance of 2.91 mH for the large copper ring. This is close to the marked value of 2.75 mH.

Part 2

Using the following equation we derive the theoretical value for phase difference to be 1.57 radians

$$\tan\phi = \frac{\omega L - 1}{\omega C}$$

Our measured value of 1.55 ± 0.0246 radians agrees within error of the derived value.

Our measured V_C las by 92 degrees which is within error an expected phase difference of 90 degrees. Out experimental value for V_L however did not agree within error to 90 degrees to a potential misread or noise in the oscilloscope.

Inductors are passive electronic components that temporarily store energy in a magnetic field. When current flows through the solenoidal coil, a magnetic field is produced. High frequencies of voltages results in the inductor resisting signals because the magnetic field does not have time to stabilize. When current is varied in an inductor, the charges accumulate within

the inductor resulting in it behaving like a resistor. On the other hand, a capacitor is able to continuously charge and discharge make it useful for high frequency AC signals and more resistant to DC current.

Finally we note that we observed the behavior of the capacitor and inductor indirectly, by looking at the signal across the resistor. This is because Ohm's Law ($V = IR$) allows us to relate changing behavior in the resistor to the changing voltage.

4 Conclusion

In this lab we observe the behavior of an RLC circuit by once again using an oscilloscope. In Part 1 we find observe resonance frequency and record peak-to-peak voltage as a function of frequency. We do multiple trials with three values of resistance. Our calculated resonance frequencies agreed within error of expected values. In part 2 we observe phase differences in the resistor, inductor, and capacitor. Our experimental values for resistor and capacitance agreed within uncertainties.

After the completion of this lab we have come to fully understand how oscilloscopes are useful tools measuring numerous types of circuits. Through observing properties of RLC circuits we have gained a better understanding physically and intuitively of resonance frequency and phase difference.

5 Code

Absorption of Beta Rays and Gamma Rays (Revised Dec 2023)

Author: Tiffany Fu / Lab Members: Anvita Bansal, Alexandria Lam

1 Introduction

On March 1896, French physicist Henri Becquerel completed an experiment and discovered that uranium salts emitted radiation. In 1898 French physicists Pierre and Marie Curie discovered the strongly radioactive elements polonium and radium.

In this lab we study the behavior of beta (β) and gamma (γ) rays as they pass through matter. In Part 1, we measure the range of β-particles from a given source and derive the endpoint energy of decay. In beta decay, an energized electron (a beta particle) is emitted. When a beta particle traverses matter, it will give electrostatic impulses to nearby electrons and thus ionize atoms in the material. Because of its ionizing action, an incident particle in matter will continuously lose kinetic energy, eventually coming to rest after traversing a path length called its range.The incident electron range can not be sharply determined but in this experiment we use the following approximation where E is mass-energy (the energy used to create decay products) and ρ is the density of the stopping material.

$$r = \frac{0.412 g \mathrm{cm}^{-2}}{\rho} E^{1.29}$$

Fig. 1: Approximation for Incident Electron Range r

In Part 2, we observe gamma radiation in order to determine the absorption coefficient in lead. Gamma rays are electromagnetic radiation but their energies are so high that they effectively behave like particles. Gamma rays are electrically neutral, so they do not ionize matter but instead interact with absorbers in one of three ways: compton scattering, photoelectric effect, or pair production. The total probability that a gamma ray will interact with a block of material is described by the linear absorption coefficient of the material μ. μ is defined by the equation

$$\frac{dN}{dx} = -\mu N$$

With the solution

$$N(x) = N_0 e^{-\mu x}$$

2 Method

Part 1: Beta Rays

Our experimental we use a Geiger counter to observe particles emitted from radioactive nuclei. By setting up a basic Geiger current, we create implement the Townsend avalanche process to count the number of charged particles entering the chamber.

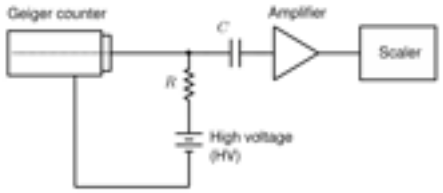

Fig. 2: Geiger Counter Circuit

We begin by setting up our Geiger counter. We calibrate the working voltage to a plateau region, a region where the counting rate is relatively insensitive to changes in the high voltage (HV) supply. Our counter plateaued around 870 Volts which we set as HV for the remainder of our experiment.

Voltage (V)	Count
650	0
660	1
670	22
690	249
710	1283
730	2489
750	2710
770	2841
790	2782
810	2912
830	2947
850	2983
870	3109

Tab. 1: Geiger Counter Calibration Results

We use the unstable isotope Thallium-204 to generate beta particles in the next step of our experiment. We place our Thallium source on the second shelf of our detector. We then record the counting rate and sheets of aluminum foil until the counting rate reaches our background level of 19. To measure statistical error, we use the error of a Poisson distribution: $1\sqrt{N}$.

Sheets	Counting Rate	Error
0	243	0.064
1	173	0.076
2	128	0.088
3	82	0.110
4	73	0.117
5	44	0.151
6	39	0.160
7	29	0.186
8	25	0.200
9	23	0.209
10	22	0.213

Tab. 2: Counting Rate and Error or Beta Particles with Thallium-204 Decay

Part 2: Gamma Rays To observe γ-rays our radioactive source is Cesium-137 which decays with a half-life of 30 years to Barium-137. We once again record the absorption curve this time using lead sheets.

Sheets	Counting Rate	Error
0	125.5	0.089
1	134	0.086
2	104	0.098
3	91	0.105
4	88	0.107
5	73	0.117
6	59	0.130

Tab. 3: Counting Rate and Error or Gamma Particles with Celsium-137 Decay

3 Analysis & Results

Part 1: Beta Rays First, we make a semi-log plot of the counts versus the absorber thickness. Note that the thickness of our aluminum sheets is 2 mils.

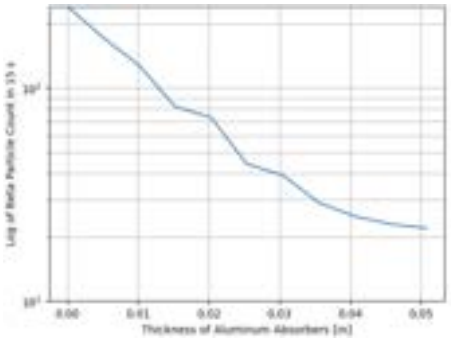

Fig. 3: Beta Ray Absorption Curve

Using our plot and extrapolating we determine a maximum range of 0.05 inches or 0.127 centimeters.

Our expected value for range is calculated using our derived equation and a E of 0.765 and ρ of 2.702 g cm^3.

$$r = \frac{0.412 g \text{cm}^{-2}}{2.702} 0.765^{1.29} = 0.113$$

Our values were not very similar since we did not complete trials for more than 10 aluminum sheets. If we completed more trials we could've observed a greater and more accurate value of range for beta rays.

Part 2: Gamma Rays For our second plot we first linearize our data by taking the natural log of count data and then plot them against lead thickness.

Thickness	ln(Counting Rate)
0	4.832
0.062	4.898
0.124	4.644
0.186	4.511
0.248	4.477
0.31	4.290
0.372	4.078

Tab. 4: Absorption Thickness and Natural Log of Counting Rate

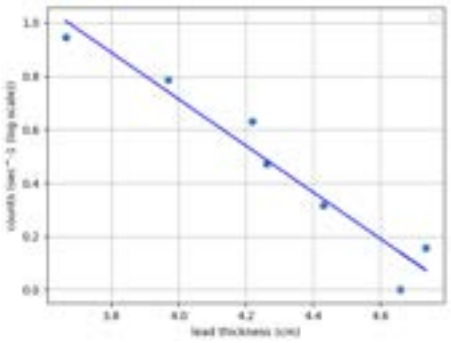

Fig. 4: Absorption Curve of Gamma Rays

After performing a linear fit, we find the absorption coefficient μ from the slope 0.872 ± 0.04199.

Using this result and the following figure we estimate the energy of the gamma rays to be 0.900 MeV.

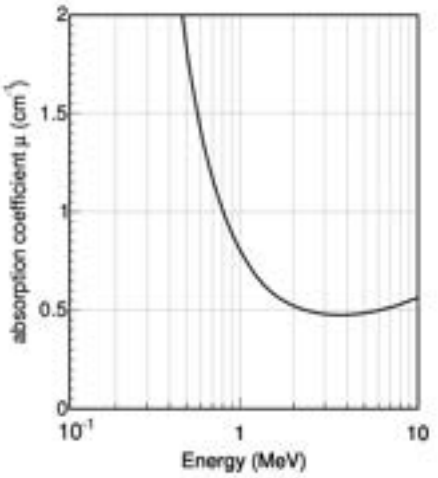

Fig. 5: Linear Absorption Coefficient for γ Rays in Lead as a Function of Energy

The accepted value of the energy of gamma rays is 0.662 MeV, our predicted value does not agree within error. This is likely due to factors that limit the precision of our estimate namely the precision of our Geiger counter. The efficiency of the Geiger counter is much lower for γ rays as compared to α or β particles. This is because gamma rays have a low probability of interacting with common materials so most gamma rays

will pass undetected. Gamma rays also travel in all directions so rays may not directly pass the chamber. In future experiments we may consider using other methods of gamma spectroscopy such as a scintillation detector or a semiconductor. In detecting alpha rays a spark detector is often used and for beta rays liquid scintillation is a common method.

4 Conclusion

To conclude our final lab we observed the behavior of beta and gamma rays passing through matter. By recording count and absorption thickness we plotted absorption curves for beta and gamma rays. Through the analysis of respective plots we find the incident electron range of β-particles (0.127 cm) and energy level of γ rays (0.900 MeV). Compared to expected values, our experimental values were close but not accurate within uncertainties. We note potential improvements to increase accuracy in measuring radioactive rays especially gamma rays.

Throughout the past semester of lab experiments we have continuously built on top of our physical understanding. From mechanics, electromagnetism, circuits, to radiation: we have gained a deep understanding of the laws of physics and the tools scientists use to observe them.

5 Code

```
import pandas as pd
import matplotlib.pyplot as plt
import numpy as np
from scipy.stats import linregress

df = pd.read_csv('lab10b.csv')

thicc = df['Aluminum_Thickness']
count = df['Beta_Count']

plt.grid(True, which="both")
plt.semilogy(thicc, count)
plt.ylim([10,243])

plt.xlabel('Thickness of Aluminum Absorbers [in]')
plt.ylabel('Log of Beta Particle Count in 15 s')

plt.show()

thickness = np.array([0, 0.15748, 0.31496, 0.47244, 0.62992, 0.7874, 0.94488])  # X values

count = np.array([4.658710953, 4.736198448, 4.430816799, 4.262679877, 4.219507705, 3.970291914, 3.66356164

plt.scatter(count, thickness)
slope, intercept = np.polyfit(count, thickness, 1)
plt.plot(count, slope * count + intercept, color='blue')

plt.ylabel('counts (sec^-1 (log scale))')
plt.xlabel('lead thickness (cm)')
plt.legend()


slope, intercept, r_value, p_value, std_err = linregress(count, thickness)

slope_error = std_err / np.sqrt(6)

print(f"Slope = {slope:.3f} ± {slope_error:.5f}")

plt.grid(True)
plt.show()
```